

THE KINETIC THEORY OF DILUTE SOLUTIONS OF FLEXIBLE POLYMERS: HYDRODYNAMIC INTERACTION

J. Ravi Prakash^a

^aDepartment of Chemical Engineering, Indian Institute of Technology, Madras, India, 600 036

1. INTRODUCTION

The rheological properties of dilute polymer solutions are commonly used in industry for characterising the dissolved polymer in terms of its molecular weight, its mean molecular size, its chain architecture, the relaxation time spectrum, the translational diffusion coefficient and so on. There is therefore considerable effort world wide on developing molecular theories that relate the microscopic structure of the polymer and its interactions with the solvent to the observed macroscopic behavior. In this chapter, recent theoretical progress that has been made in the development of a coherent conceptual framework for modelling the rheological properties of dilute polymer solutions is reviewed.

A polymer solute molecule dissolved in a dilute Newtonian solvent is typically represented in molecular theories by a coarse-grained mechanical model, while the relatively rapidly varying motions of solvent molecules surrounding the polymer molecule are replaced by a random force field acting on the mechanical model. The replacement of the complex polymer molecule with a coarse-grained mechanical model is justified by the belief that such models capture those large scale properties of the polymer molecule, such as its stretching and orientation by the solvent flow field, that are considered to be responsible for the solution's macroscopic behavior. An example of a coarse-grained model frequently used to represent a flexible polymer molecule is the *bead-spring chain*, which is a linear chain of identical beads connected by elastic springs.

Progress in the development of molecular theories for dilute polymer solutions has essentially involved the successive introduction, at the molecular level, of various physical phenomena that are considered to be responsible for the macroscopic properties of the polymer solution. For instance, the simplest theory based on a bead-spring model assumes that the solvent influences the motion of the beads by exerting a drag force and a Brownian force. Since this theory fails to predict a large number of the observed features of polymer solutions, more advanced theories have been developed which incorporate additional microscopic phenomena. Thus, theories have been developed which (i) include the phenomenon of 'hydrodynamic interaction' between the beads, (ii) try to account for the finite extensibility of the polymer molecule, (iii) attempt to ensure that two parts of the polymer chain do not occupy the same place at the same time, (iv) consider the internal friction experienced when two parts of a polymer chain close to each other in space move apart, and so on. The aim of this chapter is to present the unified framework within which these microscopic phenomena may be treated, and to focus in particular on recent advances in the treatment of the effect of hydrodynamic interaction. To a large extent, the notation that is used here is the same as that in the treatise *Dynamics of Polymeric Liquids* by Bird and co-authors [2].

2. TRANSPORT PROPERTIES OF DILUTE SOLUTIONS

2.1. Dilute solutions

A solution is considered dilute if the polymer chains are isolated from each other and have negligible interactions with each other. In this regime of concentration the polymer solution's properties are determined by the nature of the interaction between the segments of a single polymer chain with each other,

and by the nature of the interaction between the segments and the surrounding solvent molecules. As the concentration of polymers is increased, a new threshold is reached where the polymer molecules begin to interpenetrate and interact with each other. This threshold is reached at a surprisingly low concentration, and heralds the inception of the semi-dilute regime, where the polymer solution's properties have been found to be significantly different. Beyond the semi-dilute regime lie concentrated solutions and melts. In this chapter we are concerned exclusively with the behavior of dilute solutions.

A discussion of the threshold concentration at which the semi-dilute regime is initiated is helpful in introducing several concepts that are used frequently in the description of polymer solutions.

A polymer molecule surrounded by solvent molecules undergoes thermal motion. A measure of the average size of the polymer molecule is the root mean square distance between the two ends of the polymer chain, typically denoted by R . This size is routinely measured with the help of scattering experiments, and is found to increase with the molecular weight of the polymer chain with a scaling law, $R \sim M^\nu$, where M is the molecular weight, and ν is the scaling exponent which depends on the nature of the polymer-solvent interaction. In *good* solvents, solute-solvent interactions are favoured relative to solute-solute interactions. As a consequence the polymer chain *swells* and its size is found to scale with an exponent $\nu = 3/5$. On the other hand, in *poor* solvents, the situation is one in which solute-solute interactions are preferred. There exists a particular temperature, called the *theta* temperature, at which the scaling exponent ν changes dramatically from $3/5$ to $1/2$. At this temperature, the urge to expand caused by two parts of the chain being unable to occupy the same location (leading to the presence of an *excluded volume*), is just balanced by the repulsion of the solute molecules by the solvent molecules.

Polymer chains in a solution can be imagined to begin to interact with each other when the solution volume is filled with closely packed spheres representing the average size of the molecule. This occurs when $n_p R^3 \approx 1$, where n_p is the number of chains per unit volume. Since $n_p = \rho_p N_A / M$, where ρ_p is the polymer mass density and N_A is Avagadro's number, it follows that polymer density at overlap, ρ_p^* , scales with molecular weight as, $\rho_p^* \sim M^{1-3\nu}$. Polymer molecules typically have molecular weights between 10^4 and 10^6 gm/mol. As a result, it is clear that the polymer solution can be considered dilute only at very low polymer densities. Since experimental measurements are difficult at such low concentrations, the usual practice is to extrapolate results of experiments carried out at decreasing concentrations to the limit of zero concentration. For instance, in the case of dilute polymer solutions it is conventional to report the *intrinsic* viscosity, which is defined by,

$$[\eta] = \lim_{\rho_p \rightarrow 0} \frac{\eta_p}{\rho_p \eta_s} \quad (1)$$

where η_p is the polymer contribution to the solution viscosity, and η_s is the solvent viscosity.

2.2. Homogeneous flows

Complex flow situations typically encountered in polymer processing frequently involve a combination of shearing and extensional deformations. The response of the polymer solution to these two modes of deformation is very different. Consequently, predicting the rheological properties of the solution under both shear and extensional deformation is considered to be very important in order to properly characterise the solutions behavior. Rather than considering flows where both these modes of deformation are simultaneously present, it is common in polymer kinetic theory to analyse simpler flow situations called *homogeneous* flows, where they may be treated separately.

A flow is called homogeneous, if the rate of strain tensor, $\dot{\gamma} = (\nabla \mathbf{v})(t) + (\nabla \mathbf{v})^\dagger(t)$, where \mathbf{v} is the solution velocity field, is independent of position. In other words, the solution velocity field \mathbf{v} in homogeneous flows, can always be represented as $\mathbf{v} = \mathbf{v}_0 + \boldsymbol{\kappa}(t) \cdot \mathbf{r}$, where \mathbf{v}_0 is a constant vector, $\boldsymbol{\kappa}(t) = \nabla \mathbf{v}(t)$ is a traceless tensor for incompressible fluids, and \mathbf{r} is the position vector with respect to a laboratory fixed frame of reference. While there is no spatial variation in the rate of strain tensor in homogeneous flows, there is no restriction with regard to its variation in time. Therefore, the response of dilute solutions to *transient* shear and extensional flows is also used to probe its character as an alternative means of characterisation independent of the steady state material functions.

Two homogeneous flows, steady simple shear flow and small amplitude oscillatory shear flow, that are frequently used to validate the predictions of molecular theories which incorporate hydrodynamic interaction, are described briefly below. A comprehensive discussion of material functions in various flow situations can be found in the book by Bird *et al.* [1].

2.3. Simple shear flows

The rheological properties of a dilute polymer solution can be obtained once the stress tensor, $\boldsymbol{\tau}$, is known. The stress tensor is considered to be given by the sum of two contributions, $\boldsymbol{\tau} = \boldsymbol{\tau}^s + \boldsymbol{\tau}^p$, where $\boldsymbol{\tau}^s$ is the contribution from the solvent, and $\boldsymbol{\tau}^p$ is the polymer contribution. Since the solvent is assumed to be Newtonian, the solvent stress (using a compressive definition for the stress tensor [1]) is given by, $\boldsymbol{\tau}^s = -\eta_s \dot{\boldsymbol{\gamma}}$. The nature of the polymer contribution $\boldsymbol{\tau}^p$ in simple shear flows is discussed below.

Simple shear flows are described by a velocity field,

$$v_x = \dot{\gamma}_{yx} y, v_y = 0, v_z = 0 \quad (2)$$

where the velocity gradient $\dot{\gamma}_{yx}$ can be a function of time. From considerations of symmetry, one can show that the most general form that the polymer contribution to the stress tensor can have in simple shear flows is [1],

$$\boldsymbol{\tau}^p = \begin{pmatrix} \tau_{xx}^p & \tau_{xy}^p & 0 \\ \tau_{xy}^p & \tau_{yy}^p & 0 \\ 0 & 0 & \tau_{zz}^p \end{pmatrix} \quad (3)$$

where the matrix of components in a Cartesian coordinate system is displayed. The form of the stress tensor implies that only three independent combinations can be measured for an incompressible fluid. All simple shear flows are consequently characterised by three material functions.

2.3.1. Steady simple shear flows

Steady simple shear flows are described by a constant shear rate, $\dot{\gamma} = |\dot{\gamma}_{yx}|$. The tensor $\boldsymbol{\kappa}$ is consequently given by the following matrix representation in the laboratory-fixed coordinate system,

$$\boldsymbol{\kappa} = \dot{\gamma} \begin{pmatrix} 0 & 1 & 0 \\ 0 & 0 & 0 \\ 0 & 0 & 0 \end{pmatrix} \quad (4)$$

The three independent material functions used to characterize such flows are the viscosity, η_p , and the first and second normal stress difference coefficients, Ψ_1 and Ψ_2 , respectively. These functions are defined by the following relations,

$$\tau_{xy}^p = -\dot{\gamma} \eta_p; \quad \tau_{xx}^p - \tau_{yy}^p = -\dot{\gamma}^2 \Psi_1; \quad \tau_{yy}^p - \tau_{zz}^p = -\dot{\gamma}^2 \Psi_2 \quad (5)$$

where $\tau_{xy}^p, \tau_{xx}^p, \tau_{yy}^p$ are the components of the polymer contribution to the stress tensor $\boldsymbol{\tau}^p$.

At low shear rates, the viscosity and the first normal stress coefficient are observed to have constant values, $\eta_{p,0}$ and $\Psi_{1,0}$, termed the zero shear rate viscosity and the zero shear rate first normal stress coefficient, respectively. At these shear rates the fluid is consequently Newtonian in its behavior.

At higher shear rates, most dilute polymer solutions show *shear thinning* behavior. The viscosity and the first normal stress coefficient decrease with increasing shear rate, and exhibit a pronounced *power law* region. At very high shear rates, the viscosity has been observed to level off and approach a constant value, $\eta_{p,\infty}$, called the infinite shear rate viscosity. A high shear rate limiting value has not been observed for the first normal stress coefficient. The second normal stress coefficient is much smaller in magnitude than the first normal stress coefficient, however its sign has not been conclusively established experimentally. Note that the normal stress differences are zero for a Newtonian fluid. The existence of non-zero normal stress differences is an indication that the fluid is viscoelastic.

Experiments with very high molecular weight systems seem to suggest that polymer solutions can also *shear thicken*. It has been observed that the viscosity passes through a minimum with increasing shear rate, and then increases until a plateau region before shear thinning again [17].

It is appropriate here to note that shear flow material functions are usually displayed in terms of the reduced variables, $\eta_p/\eta_{p,0}$, $\Psi_1/\Psi_{1,0}$ and Ψ_2/Ψ_1 , versus a non-dimensional shear rate β , which is defined by $\beta = \lambda_p \dot{\gamma}$, where, $\lambda_p = [\eta]_0 M \eta_s / N_A k_B T$, is a characteristic relaxation time. The subscript 0 on the square bracket indicates that this quantity is evaluated in the limit of vanishing shear rate, k_B is Boltzmann's constant and T is the absolute temperature. For dilute solutions one can show that, $[\eta]/[\eta]_0 = \eta_p/\eta_{p,0}$ and $\beta = \eta_{p,0} \dot{\gamma} / n_p k_B T$.

2.3.2. Small amplitude oscillatory shear flow

A transient experiment that is used very often to characterise polymer solutions is *small amplitude oscillatory shear flow*. The upper plate in a simple shear experiment is made to undergo sinusoidal oscillations in the plane of flow with frequency ω . For oscillatory flow between narrow slits, the shear rate at any position in the fluid is given by [1], $\dot{\gamma}_{yx}(t) = \dot{\gamma}_0 \cos \omega t$, where $\dot{\gamma}_0$ is the amplitude. The tensor $\kappa(t)$ is consequently given by,

$$\kappa(t) = \dot{\gamma}_0 \cos \omega t \begin{pmatrix} 0 & 1 & 0 \\ 0 & 0 & 0 \\ 0 & 0 & 0 \end{pmatrix} \quad (6)$$

Since the polymer contribution to the shear stress in oscillatory shear flow, τ_{yx}^p , undergoes a phase shift with respect to the shear strain and the strain rate, it is customary to represent its dependence on time through the relation [1],

$$\tau_{yx}^p = -\eta'(\omega) \dot{\gamma}_0 \cos \omega t - \eta''(\omega) \dot{\gamma}_0 \sin \omega t \quad (7)$$

where η' and η'' are the material functions characterising oscillatory shear flow. It is common to represent them in a combined form as the complex viscosity, $\eta^* = \eta' - i\eta''$.

Two material functions which are entirely equivalent to η' and η'' and which are often used to display experimental data, are the storage modulus $G' = \omega\eta'/(nk_B T)$ and the loss modulus $G'' = \omega\eta''/(nk_B T)$. Note that the term involving G' in equation(7) is in phase with the strain while that involving G'' is in phase with the strain rate. For an elastic material, $G'' = 0$, while for a Newtonian fluid, $G' = 0$. Thus, G' and G'' are measures of the extent of the fluid's viscoelasticity.

In flow situations which have a small displacement gradient, termed the *linear viscoelastic* flow regime, the stress tensor in polymeric fluids is described by the linear constitutive relation,

$$\tau^p = - \int_{-\infty}^t ds G(t-s) \dot{\gamma}(t,s) \quad (8)$$

where $G(t)$ is the relaxation modulus.

When the amplitude $\dot{\gamma}_0$ is very small, oscillatory shear flow is a linear viscoelastic flow and consequently can also be described in terms of a relaxation modulus $G(t)$. Indeed, expressions for the real and imaginary parts of the complex viscosity can be found from the expression,

$$\eta^* = \int_0^\infty G(s) e^{-i\omega s} ds \quad (9)$$

Experimental plots of $\log G'$ and $\log G''$ versus nondimensional frequency show three distinct power law regimes. The regime of interest is the intermediate regime [17], where for dilute solutions of high molecular weight polymers in good or theta solvents, both G' and G'' have been observed to scale with frequency as $\omega^{2/3}$.

It is appropriate to note here that the zero shear rate viscosity $\eta_{p,0}$ and the zero shear rate first normal stress difference $\Psi_{1,0}$, which are linear viscoelastic properties, can be obtained from the complex viscosity in the limit of vanishing frequency,

$$\eta_{p,0} = \lim_{\omega \rightarrow 0} \eta'(\omega); \quad \Psi_{1,0} = \lim_{\omega \rightarrow 0} \frac{2\eta''(\omega)}{\omega} \quad (10)$$

2.4. Scaling with molecular weight

We have already discussed the scaling of the root mean square end-to-end distance of a polymer molecule with its molecular weight. In this section we discuss the scaling of the zero shear rate intrinsic viscosity $[\eta]_0$, and the translational diffusion coefficient D , with the molecular weight, M . As we shall see later, these have proven to be vitally important as experimental benchmarks in attempts to improve predictions of molecular theories.

It has been found that the relationship between $[\eta]_0$ and M can be expressed by the formula,

$$[\eta]_0 = K M^a \quad (11)$$

where, a is called the *Mark-Houwink* exponent, and the prefactor K depends on the polymer-solvent system. The value of the parameter a lies between 0.5 and 0.8, with the lower limit corresponding to theta conditions, and the upper limit to a good solvent with a very high molecular weight polymer solute. Measured intrinsic viscosities are routinely used to determine the molecular weight of samples once the constants K and a are known for a particular polymer-solvent pair.

The translational diffusion coefficient D for a flexible polymer in a dilute solution can be measured by dynamic light scattering methods, and is found to scale with molecular weight as [2],

$$D \sim M^{-\mu} \quad (12)$$

where the exponent μ lies in the range 0.49 to 0.6. Most theta solutions have values of μ close to the lower limit. On the other hand, there is wide variety in the value of μ reported for good solvents. It appears that the upper limit is attained only for very large molecular weight polymers and the intermediate values, corresponding to a *cross over* region, are more typical of real polymers with moderate molecular weights.

2.5. Universal behavior

It is appropriate at this point to discuss the most important aspect of the behavior of polymer solutions (as far as the theoretical modelling of these solutions is concerned) that is revealed by the various experimental observations. When the experimental data for high molecular weight systems is plotted in terms of appropriately normalized coordinates, the most noticeable feature is the exhibition of *universal* behavior. By this it is meant that curves for different values of a parameter, such as the molecular weight, the temperature, or even for different types of monomers can be superposed onto a single curve. For example, when the reduced intrinsic viscosity, $[\eta]/[\eta]_0$ is plotted as a function of the reduced shear rate β , the curves for polystyrene in different types of good solvents at various temperatures collapse onto a single curve [1].

There is, however, an important point that must be noted. While polymers dissolved in both theta solvents and good solvents show universal behavior, the universal behavior is different in the two cases. An example of this is the observed scaling behavior of various quantities with molecular weight. The scaling is universal within the context of a particular type of solvent. The term *universality class* is used to describe the set of systems that exhibit common universal behavior [40]. Thus theta and good solvents belong to different universality classes.

The existence of universality classes is very significant for the theoretical description of polymer solutions. Any attempt made at modelling a polymer solution's properties might expect that a proper description must incorporate the chemical structure of the polymer into the model, since this determines its microscopic behavior. Thus a detailed consideration of bonds, sidegroups, *etc.* may be envisaged.

However, the universal behavior that is revealed by experiments suggests that macroscopic properties of the polymer solution are determined by a few large scale properties of the polymer molecule. Structural details may be ignored since at length scales in the order of nanometers, different polymer molecules become equivalent to each other, and behave in the same manner. As a result, polymer solutions that differ from each other with regard to the chemical structure or molecular weight of the polymer molecules that are dissolved in it, the temperature, and so on, still behave similarly as long as a few parameters that describe molecular features are the same.

This universal behavior justifies the introduction of crude mechanical models, such as the bead-spring chain, to represent real polymer molecules. On the other hand, it is interesting to note that in many cases, the predictions of these models are not universal. It turns out that apart from a basic length and time scale, there occur other parameters that need to be prescribed, for example, the number of beads N in the chain, the strength of hydrodynamic interaction h^* , the finite spring extensibility parameter b , and so on. It is perhaps not incorrect to state that any molecular theory that is developed must ultimately verify that universal predictions of transport properties are indeed obtained. The universal predictions of kinetic theory models with hydrodynamic interaction are discussed later on in this chapter.

3. BEAD-SPRING CHAIN MODELS

The development of a kinetic theory for dilute solutions has been approached in two different ways. One of them is an intuitive approach in the configuration space of a single molecule, with a particular mechanical model chosen to represent the macromolecule, such as a freely rotating bead-rod chain or a freely jointed bead-spring chain [13, 36, 45]. The other approach is to develop a formal theory in the phase space of the entire solution, with the polymer molecule represented by a general mechanical model that may have internal constraints, such as constant bond lengths and angles [16, 5, 2]. The results of the former method are completely contained within the latter method, and several ad hoc assumptions made in the intuitive treatment are clarified and placed in proper context by the development of the rigorous phase space theory. Kinetic theories developed for *flexible* macromolecules in dilute solutions have generally pursued the intuitive approach, with the bead-spring model proving to be the most popular. This is because the lack of internal constraints in the model makes the formulation of the theory simpler. Recently, Curtiss and Bird [4], acknowledging the ‘notational and mathematical’ complexity of the rigorous phase space theory for general mechanical models, have summarised the results of phase space theory for the special case of bead-spring models with arbitrary connectivity, *ie.* for linear chains, rings, stars, combs and branched chains.

In this section, since we are primarily concerned with reviewing recent developments in theories for flexible macromolecules, we describe the development of kinetic theories in the configuration space of a single molecule. However, readers who wish to understand the origin of the ad hoc expressions used for the Brownian forces and the hydrodynamic force, and the formal development of expressions for the momentum and mass flux, are urged to read the article by Curtiss and Bird [4].

The general diffusion equation that governs the time evolution of the distribution of configurations of a bead-spring chain subject to various nonlinear effects, and the microscopic origin of the polymer contribution to the stress tensor are discussed in this section. The simplest bead-spring chain model, the *Rouse* model is also discussed. We begin, however, by describing the equilibrium statistical mechanical arguments that justify the representation of a polymer molecule with a bead-spring chain model, and we discuss the equilibrium configurations of such a model.

3.1. Equilibrium configurations

When a flexible polymer chain in a *quiescent* dilute solution is considered at a lowered resolution, *ie.* at a coarse-grained level, it would appear like a strand of highly coiled spaghetti, and the extent of its coiling would depend on its degree of flexibility. A quantity used to characterise a chain’s flexibility is the *orientational correlation function*, whose value $K_{or}(\Delta\ell)$, is a measure of the correlation in the direction of the chain at two different points on the chain which are separated by a distance $\Delta\ell$ along the length

of the chain. At sufficiently large distances $\Delta\ell$, it is expected that the correlations vanish. However, it is possible to define a *persistence length* ℓ_{ps} , such that for $\Delta\ell > \ell_{ps}$, orientational correlations are negligible [40].

The existence of a persistence length suggests that as far as the global properties of a flexible polymer chain are concerned, such as the distribution function for the end-to-end distance of the chain, the continuous chain could be replaced by a freely jointed chain made up of rigid links connected together at joints that are completely flexible, whose linear segments are each longer than the persistence length ℓ_{ps} , and whose contour length is the same as that of the continuous chain.

The freely jointed chain undergoing thermal motion is clearly analogous to a random-walk in space, with each random step in the walk representing a link in the chain assuming a random orientation. Thus all the statistical properties of a random-walk are, by analogy, also the statistical properties of the freely jointed chain. The equivalence of a polymer chain with a random-walk lies at the heart of a number of fundamental results in polymer physics.

3.1.1. Distribution functions and averages

In polymer kinetic theory, the freely jointed chain is assumed to have beads at the junction points between the links, and is referred to as the freely jointed bead-rod chain [2]. The introduction of the beads is to account for the mass of the polymer molecule and the viscous drag experienced by the polymer molecule. While in reality the mass and drag are distributed continuously along the length of the chain, the model assumes that the total mass and drag may be distributed over a finite number of discrete beads.

For a general chain model consisting of N beads, which have position vectors \mathbf{r}_ν , $\nu = 1, 2, \dots, N$, in a laboratory fixed coordinate system, the Hamiltonian is given by,

$$\mathcal{H} = \mathcal{K} + \phi(\mathbf{r}_1, \mathbf{r}_2, \dots, \mathbf{r}_N) \quad (13)$$

where \mathcal{K} is the kinetic energy of the system and ϕ is the potential energy. ϕ depends on the location of all the particles.

The center of mass \mathbf{r}_c of the chain, and its velocity $\dot{\mathbf{r}}_c$ are given by

$$\mathbf{r}_c = \frac{1}{N} \sum_{\nu=1}^N \mathbf{r}_\nu \quad ; \quad \dot{\mathbf{r}}_c = \frac{1}{N} \sum_{\nu=1}^N \dot{\mathbf{r}}_\nu \quad (14)$$

where $\dot{\mathbf{r}}_\nu = d\mathbf{r}_\nu/dt$. The location of a bead with respect to the center of mass is specified by the vector $\mathbf{R}_\nu = \mathbf{r}_\nu - \mathbf{r}_c$.

If Q_1, Q_2, \dots, Q_d denote the generalised internal coordinates required to specify the configuration of the chain, then the kinetic energy of the chain in terms of the velocity of the center of mass and the generalised velocities $\dot{Q}_s = dQ_s/dt$, is given by [2],

$$\mathcal{K} = \frac{mN}{2} \dot{\mathbf{r}}_c^2 + \frac{1}{2} \sum_s \sum_t g_{st} \dot{Q}_s \dot{Q}_t \quad (15)$$

where the indices s and t vary from 1 to d , m is the mass of a bead, and g_{st} is the *metric matrix*, defined by, $g_{st} = m \sum_\nu (\partial \mathbf{R}_\nu / \partial Q_s) \cdot (\partial \mathbf{R}_\nu / \partial Q_t)$. In terms of the momentum of the center of mass, $\mathbf{p}_c = mN \dot{\mathbf{r}}_c$, and the generalised momenta P_s , defined by, $P_s = (\partial \mathcal{K} / \partial \dot{Q}_s)$, the kinetic energy has the form [2],

$$\mathcal{K} = \frac{1}{2mN} \mathbf{p}_c^2 + \frac{1}{2} \sum_s \sum_t G_{st} P_s P_t \quad (16)$$

where, G_{st} are the components of the matrix inverse to the metric matrix, $\sum_t G_{st} g_{tu} = \delta_{su}$, and δ_{su} is the Kronecker delta.

The probability, $\mathcal{P}_{\text{eq}} d\mathbf{r}_c dQ d\mathbf{p}_c dP$, that an N -bead chain model has a configuration in the range $d\mathbf{r}_c dQ$ about \mathbf{r}_c, Q and momenta in the range $d\mathbf{p}_c dP$ about \mathbf{p}_c, P is given by,

$$\mathcal{P}_{\text{eq}}(\mathbf{r}_c, Q, \mathbf{p}_c, P) = \mathcal{Z}^{-1} e^{-\mathcal{H}/k_{\text{B}}T} \quad (17)$$

where \mathcal{Z} is the *partition function*, defined by,

$$\mathcal{Z} = \int \int \int \int e^{-\mathcal{H}/k_{\text{B}}T} d\mathbf{r}_c dQ d\mathbf{p}_c dP \quad (18)$$

The abbreviations, Q and dQ have been used to denote Q_1, Q_2, \dots, Q_d and $dQ_1 dQ_2 \dots dQ_d$, respectively, and a similar notation has been used for the momenta.

The *configurational distribution function* for a general N -bead chain, $\psi_{\text{eq}}(Q) dQ$, which gives the probability that the internal configuration is in the range dQ about Q , is obtained by integrating \mathcal{P}_{eq} over all the momenta and over the coordinates of the center of mass,

$$\psi_{\text{eq}}(Q) = \mathcal{Z}^{-1} \int \int \int e^{-\mathcal{H}/k_{\text{B}}T} d\mathbf{r}_c d\mathbf{p}_c dP \quad (19)$$

For an N -bead chain whose potential energy does not depend on the location of the center of mass, the following result is obtained by carrying out the integrations over \mathbf{p}_c and P [2],

$$\psi_{\text{eq}}(Q) = \frac{\sqrt{g(Q)} e^{-\phi(Q)/k_{\text{B}}T}}{\int \sqrt{g(Q)} e^{-\phi(Q)/k_{\text{B}}T} dQ} \quad (20)$$

where, $g(Q) = \det(g_{st}) = 1/\det(G_{st})$.

An expression that is slightly different from the random-walk distribution is obtained on evaluating the right hand side of equation (20) for a freely jointed bead-rod chain. Note that the random-walk distribution is obtained by assuming that each link in the chain is oriented independently of all the other links, and that all orientations of the link are equally likely. On the other hand, equation (20) suggests that the probability for the links in a freely jointed chain being perpendicular to each other, for a given solid angle, is slightly larger than the probability of being in the same direction. In spite of this result, the configurational distribution function for a freely jointed bead-rod chain is almost always assumed to be given by the random-walk distribution [2]. Here afterwards in this chapter, we shall refer to a freely jointed bead-rod chain whose configurational distribution function is assumed to be given by the random-walk distribution, as an *ideal* chain. For future reference, note that the random-walk distribution is given by,

$$\psi_{\text{eq}}(\theta_1, \dots, \theta_{N-1}, \phi_1, \dots, \phi_{N-1}) = \left(\frac{1}{4\pi}\right)^{N-1} \prod_{i=1}^{N-1} \sin \theta_i \quad (21)$$

where θ_i and ϕ_i are the polar angles for the i th link in the chain [2].

Since the polymer chain explores many states in the duration of an observation quantities observed on macroscopic length and time scales are *averages* of functions of the configurations and momenta of the polymer chain. A few definitions of averages are now introduced that are used frequently subsequently in the chapter.

The average value of a function $X(\mathbf{r}_c, Q, \mathbf{p}_c, P)$, defined in the phase space of a polymer molecule is given by,

$$\langle X \rangle_{\text{eq}} = \int \int \int \int X \mathcal{P}_{\text{eq}} d\mathbf{r}_c dQ d\mathbf{p}_c dP \quad (22)$$

We often encounter quantities X that depend only on the internal configurations of the polymer chain and not on the center of mass coordinates or momenta. In addition, if the potential energy of the chain does

not depend on the location of the center of mass, then it is straight forward to see that the equilibrium average of X is given by,

$$\langle X \rangle_{\text{eq}} = \int X \psi_{\text{eq}} dQ \quad (23)$$

3.1.2. The end-to-end vector

The end-to-end vector \mathbf{r} of a general bead-rod chain can be found by summing the vectors that represent each link in the chain,

$$\mathbf{r} = \sum_{i=1}^{N-1} a \mathbf{u}_i \quad (24)$$

where a is the length of a rod, and \mathbf{u}_i is a unit vector in the direction of the i th link of the chain. Note that the components of the unit vectors \mathbf{u}_i , $i = 1, 2, \dots, N-1$, can be expressed in terms of the generalised coordinates Q [2].

The probability $P_{\text{eq}}(\mathbf{r}) d\mathbf{r}$, that the end-to-end vector of a general bead-rod chain is in the range $d\mathbf{r}$ about \mathbf{r} can be found by suitably contracting the configurational distribution function $\psi_{\text{eq}}(Q)$ [2],

$$P_{\text{eq}}(\mathbf{r}) = \int \delta\left(\mathbf{r} - \sum_i a \mathbf{u}_i\right) \psi_{\text{eq}}(Q) dQ \quad (25)$$

where $\delta(\cdot)$ represents a Dirac delta function.

With $\psi_{\text{eq}}(Q)$ given by the random-walk distribution (21), it can be shown that for large values of N and $r = |\mathbf{r}| < 0.5Na$, the probability distribution for the end-to-end vector is a Gaussian distribution,

$$P_{\text{eq}}(\mathbf{r}) = \left(\frac{3}{2\pi(N-1)a^2}\right)^{3/2} \exp\left(\frac{-3r^2}{2(N-1)a^2}\right) \quad (26)$$

The distribution function for the end-to-end vector of an *ideal* chain with a large number of beads N is therefore given by the Gaussian distribution (26).

The mean square end-to-end distance, $\langle r^2 \rangle_{\text{eq}}$, for an ideal chain can then be shown to be, $\langle r^2 \rangle_{\text{eq}} = (N-1)a^2$. This is the well known result that the root mean square of the end-to-end distance of a random-walk increases as the square root of the number of steps. In the context of the polymer chain, since the number of beads in the chain is directly proportional to the molecular weight, this result implies that $R \sim M^{0.5}$. We have seen earlier that this is exactly the scaling observed in theta solvents. Thus one can conclude that a polymer chain in a theta solvent behaves like an ideal chain.

3.1.3. The bead-spring chain

Consider an isothermal system consisting of a bead-rod chain with a constant end-to-end vector \mathbf{r} , suspended in a bath of solvent molecules at temperature T . The partition function of such a constrained system can be found by contracting the partition function in the constraint-free case,

$$\mathcal{Z}(\mathbf{r}) = \iiint \delta\left(\mathbf{r} - \sum_i a \mathbf{u}_i\right) e^{-\mathcal{H}/k_{\text{B}}T} d\mathbf{r}_c dQ d\mathbf{p}_c dP \quad (27)$$

For an N -bead chain whose potential energy does not depend on the location of the center of mass, the integrations over \mathbf{r}_c , \mathbf{p}_c and P can be carried out to give,

$$\mathcal{Z}(\mathbf{r}) = C \int \delta\left(\mathbf{r} - \sum_i a \mathbf{u}_i\right) \psi_{\text{eq}}(Q) d\mathbf{r}_c dQ \quad (28)$$

Comparing this equation with the equation for the end-to-end vector (25), one can conclude that,

$$\mathcal{Z}(\mathbf{r}) = C P_{\text{eq}}(\mathbf{r}) \quad (29)$$

In other words, the partition function of a general bead-rod chain (except for a multiplicative factor independent of \mathbf{r}) is given by $P_{\text{eq}}(\mathbf{r})$. This result is essential to establish the motivation for the introduction of the bead-spring chain model.

At constant temperature, the change in free energy accompanying a change in the end-to-end vector \mathbf{r} of a bead-rod chain, by an infinitesimal amount $d\mathbf{r}$, is equal to the work done in the process, *ie.*, $dA = \mathbf{F} \cdot d\mathbf{r}$, where \mathbf{F} is the force required for the extension. The Helmholtz free energy of a general bead-rod chain with fixed end-to-end vector \mathbf{r} can be found from equation (29),

$$A(\mathbf{r}) = -k_{\text{B}}T \ln \mathcal{Z}(\mathbf{r}) = A_0 - k_{\text{B}}T \ln P_{\text{eq}}(\mathbf{r}) \quad (30)$$

where A_0 is a constant independent of \mathbf{r} . For an ideal chain, it follows from equations (26) and (30), that a change in the end-to-end vector by $d\mathbf{r}$, leads to a change in the free energy dA , given by,

$$dA(\mathbf{r}) = \frac{3k_{\text{B}}T}{(N-1)a^2} \mathbf{r} \cdot d\mathbf{r} \quad (31)$$

Equation (31) implies that there is a *tension* \mathbf{F} in the ideal chain, $\mathbf{F} = (3k_{\text{B}}T/(N-1)a^2) \mathbf{r}$, which resists any attempt at chain extension. Furthermore, this tension is proportional to the end-to-end vector \mathbf{r} . This implies that the ideal chain acts like a *Hookean* spring, with a spring constant H given by,

$$H = \frac{3k_{\text{B}}T}{(N-1)a^2} \quad (32)$$

The equivalence of the behavior of an ideal chain to that of a Hookean spring is responsible for the introduction of the bead-spring chain model. Since long enough *sub-chains* within the ideal chain also have normally distributed end-to-end vectors, the entire ideal chain may be replaced by beads connected to each other by springs. Note that each bead in a bead-spring chain represents the mass of a sub-chain of the ideal chain, while the spring imitates the behavior of the end-to-end vector of the sub-chain.

The change in the Helmholtz free energy of an ideal chain due to a change in the end-to-end vector is purely due to entropic considerations. The internal energy, which has only the kinetic energy contribution, does not depend on the end-to-end vector. Increasing the end-to-end vector of the chain decreases the number of allowed configurations, and this change is resisted by the chain. The entropic origin of the resistance is responsible for the use of the phrase *entropic spring* to describe the springs of the bead-spring chain model.

The potential energy S , of a bead-spring chain due to the presence of Hookean springs is the sum of the potential energies of all the springs in the chain. For a bead-spring chain with N beads, this is given by,

$$S = \frac{1}{2} H \sum_{i=1}^{N-1} \mathbf{Q}_i \cdot \mathbf{Q}_i \quad (33)$$

where $\mathbf{Q}_i = \mathbf{r}_{i+1} - \mathbf{r}_i$ is the *bead connector vector* between the beads i and $i+1$. The configurational distribution function for a Hookean bead-spring chain may be found from equation (20) by substituting $\phi(Q) = S$, with the Cartesian components of the connector vectors chosen as the generalised coordinates Q_s . The number of generalised coordinates is consequently, $d = 3N - 3$, reflecting the lack of any constraints in the model. Since $g(Q)$ is a constant independent of Q for the bead-spring chain model [2], one can show that,

$$\psi_{\text{eq}}(\mathbf{Q}_1, \dots, \mathbf{Q}_{N-1}) = \prod_j \left(\frac{H}{2\pi k_{\text{B}}T} \right)^{3/2} \exp \left(\frac{-H}{2k_{\text{B}}T} \mathbf{Q}_j \cdot \mathbf{Q}_j \right) \quad (34)$$

It is clear from equation (34) that the equilibrium distribution function for each connector vector in the bead-spring chain is a Gaussian distribution, and these distributions are independent of each other. From the property of Gaussian distributions, it follows that the vector connecting any two beads in a bead-spring chain at equilibrium also obeys a Gaussian distribution.

The Hookean bead-spring chain model has the unrealistic feature that the magnitude of the end-to-end vector has no upper bound and can in fact extend to infinity. On the other hand, the real polymer molecule has a finite fully extended length. This deficiency of the bead-spring chain model is not serious at equilibrium, but becomes important in strong flows where the polymer molecule is highly extended. Improved models seek to correct this deficiency by modifying the force law between the beads of the chain such that the chain stiffens as its extension increases. An example of such a nonlinear spring force law that is very commonly used in polymer literature is the *finitely extensible nonlinear elastic* (FENE) force law [2].

3.1.4. Excluded volume

The universal behavior of polymers dissolved in theta solvents can be explained by recognising that all high molecular weight polymers dissolved in theta solvents behave like ideal chains. However, a polymer chain cannot be identical to an ideal chain since unlike the ideal chain, two parts of a polymer chain cannot occupy the same location at the same time. In the very special case of a theta solvent, the excluded volume force is just balanced by the repulsion of the solvent molecules. In the more commonly occurring case of good solvents, the excluded volume interaction acts between any two parts of the chain that are close to each other in space, irrespective of their distance from each other along the chain length, and leads to a swelling of the chain. This is a *long range interaction*, and as a result, it seriously alters the macroscopic properties of the chain. Indeed there is a qualitative difference, and this difference cannot be treated as a small perturbation from the behavior of an ideal chain [40]. Curiously enough however, all swollen chains behave similarly to each other, and modelling this universal behavior was historically one of the challenges of polymer physics [40, 44, 7, 8, 6]. Here, we very briefly mention the manner in which the problem is formulated in the case of bead-spring chains.

The presence of excluded volume causes the polymer chain to swell. However, the swelling ceases when the entropic retractive force balances the excluded volume force. The retractive force arises due to the decreasing number of conformational states available to the polymer chain due to chain expansion. This picture of the microscopic phenomenon is captured by writing the potential energy of the bead-spring chain as a sum of the spring potential energy and the potential energy due to excluded volume interactions. The excluded volume potential energy is found by summing the interaction energy over all pairs of beads μ and ν , $E = (1/2) \sum_{\substack{\mu, \nu=1 \\ \mu \neq \nu}}^N E(\mathbf{r}_\nu - \mathbf{r}_\mu)$, where $E(\mathbf{r}_\nu - \mathbf{r}_\mu)$ is a short-range function usually taken as, $E(\mathbf{r}_\nu - \mathbf{r}_\mu) = v k_B T \delta(\mathbf{r}_\nu - \mathbf{r}_\mu)$; v being the excluded volume parameter with dimensions of volume. The total potential energy of a Hookean bead-spring chain with δ -function excluded volume interactions is consequently,

$$\phi = \frac{1}{2} H \sum_{i=1}^{N-1} \mathbf{Q}_i \cdot \mathbf{Q}_i + \frac{1}{2} v k_B T \sum_{\substack{\mu, \nu=1 \\ \mu \neq \nu}}^N \delta(\mathbf{r}_\nu - \mathbf{r}_\mu) \quad (35)$$

The equilibrium configurational distribution function of a polymer chain in the presence of Hookean springs and excluded volume can be found by substituting equation (35) into equation (20), and all average properties of the chain can be found by using equation (23). Solutions to these equations in the limit of long chains have been found by using a number of approximate schemes since an exact treatment is impossible. The most accurate scheme involves the use of field theoretic and renormalisation group methods [6]. The universal scaling of a number of equilibrium properties of dilute polymer solutions with good solvents are correctly predicted by this theory. For instance, the end-to-end distance is predicted to scale with molecular weight as, $R \sim M^{0.588}$.

The spring potential in equation (35) has been derived by considering the Helmholtz free energy of an ideal chain, *ie.* under theta conditions. It seems reasonable to expect that a more accurate derivation of

the retractive force in the chain due to entropic considerations would require the treatment of a polymer chain in a good solvent. This would lead to a non-Hookean force law between the beads [7, 29]. Such non-Hookean force laws have so far not been treated in non-equilibrium theories for dilute polymer solutions with good solvents.

3.2. Non-equilibrium configurations

Unlike in the case of equilibrium solutions it is not possible to derive the phase space distribution function for non-equilibrium solutions from very general arguments. As we shall see here it is only possible to derive a partial differential equation that governs the evolution of the configurational distribution function by considering the conservation of probability in phase space, and the equation of motion for the particular model chosen. The arguments relevant to a bead-spring chain are developed below.

3.2.1. Distribution functions and averages

The phase space of a bead-spring chain with N beads can be chosen to be given by the $6N - 6$ components of the bead position coordinates, and the bead velocities such that,

$$\mathcal{P}(\mathbf{r}_1, \dots, \mathbf{r}_N, \dot{\mathbf{r}}_1, \dots, \dot{\mathbf{r}}_N, t) d\mathbf{r}_1 \dots d\mathbf{r}_N d\dot{\mathbf{r}}_1 \dots d\dot{\mathbf{r}}_N$$

is the probability that the bead-spring chain has an instantaneous configuration in the range $d\mathbf{r}_1, \dots, d\mathbf{r}_N$ about $\mathbf{r}_1, \dots, \mathbf{r}_N$, and the beads in the chain have velocities in the range $d\dot{\mathbf{r}}_1, \dots, d\dot{\mathbf{r}}_N$ about $\dot{\mathbf{r}}_1, \dots, \dot{\mathbf{r}}_N$.

The configurational distribution function Ψ , can be found by integrating \mathcal{P} over all the bead velocities,

$$\Psi(\mathbf{r}_1, \dots, \mathbf{r}_N, t) = \int \dots \int \mathcal{P} d\dot{\mathbf{r}}_1 \dots d\dot{\mathbf{r}}_N \quad (36)$$

The distribution of internal configurations ψ , is given by,

$$\psi(\mathbf{Q}_1, \dots, \mathbf{Q}_{N-1}, t) = \int \Psi'(\mathbf{r}_c, \mathbf{Q}_1, \dots, \mathbf{Q}_{N-1}, t) d\mathbf{r}_c \quad (37)$$

where, $\Psi' = \Psi$, as a result of the Jacobian relation for the configurational vectors [2],

$$\left| \frac{\partial(\mathbf{r}_1, \dots, \mathbf{r}_N)}{\partial(\mathbf{r}_c, \mathbf{Q}_1, \dots, \mathbf{Q}_{N-1})} \right| = 1$$

Note that the normalisation condition $\int \psi d\mathbf{Q}_1 d\mathbf{Q}_2 \dots d\mathbf{Q}_{N-1} = 1$ is satisfied by ψ . When the configurations of the bead-spring chain do not depend on the location of the center of mass, as in the case of homogeneous flows with no concentration gradients, $(1/V)\psi = \Psi$, where V is the volume of the solution.

The velocity-space distribution function Ξ is defined by,

$$\Xi(\mathbf{r}_1, \dots, \mathbf{r}_N, \dot{\mathbf{r}}_1, \dots, \dot{\mathbf{r}}_N, t) = \frac{\mathcal{P}}{\Psi} \quad (38)$$

Note that Ξ satisfies the normalisation condition $\int \dots \int \Xi d\dot{\mathbf{r}}_1 \dots d\dot{\mathbf{r}}_N = 1$. Under certain circumstances that are discussed later, it is common to assume that the velocity-space distribution function is Maxwellian about the mass-average solution velocity,

$$\Xi = \mathcal{N}_M \exp \left[-\frac{1}{2k_B T} \left[m(\dot{\mathbf{r}}_1 - \mathbf{v})^2 + \dots + m(\dot{\mathbf{r}}_N - \mathbf{v})^2 \right] \right] \quad (39)$$

where \mathcal{N}_M is the normalisation constant for the Maxwellian distribution. Making this assumption implies that one expects the time scales involved in equilibration processes in momentum space to be much smaller than the time scales governing relaxation processes in configuration space.

Averages of quantities which are functions of the bead positions and bead velocities are defined analogously to the those in the previous section, namely,

$$\langle X \rangle = \int \dots \int X \mathcal{P} d\mathbf{r}_1 \dots d\mathbf{r}_N d\dot{\mathbf{r}}_1 \dots d\dot{\mathbf{r}}_N \quad (40)$$

is the the phase space average of X , while the velocity-space average is,

$$\llbracket X \rrbracket = \int \int X \Xi d\dot{\mathbf{r}}_1 \dots d\dot{\mathbf{r}}_N \quad (41)$$

For quantities X that depend only on the internal configurations of the polymer chain and not on the center of mass coordinates or bead velocities,

$$\langle X \rangle = \int X \psi d\mathbf{Q}_1 d\mathbf{Q}_2 \dots d\mathbf{Q}_{N-1} \quad (42)$$

3.2.2. The equation of motion

The equation of motion for a bead in a bead-spring chain is derived by considering the forces acting on it. The total force \mathbf{F}_μ , on bead μ is, $\mathbf{F}_\mu = \sum_i \mathbf{F}_\mu^{(i)}$, where the $\mathbf{F}_\mu^{(i)}$, $i = 1, 2, \dots$, are the various intramolecular and solvent forces acting on the bead. The fundamental difference among the various molecular theories developed so far for the description of dilute polymer solutions lies in the kinds of forces $\mathbf{F}_\mu^{(i)}$ that are assumed to be acting on the beads of the chain. In almost all these theories, the acceleration of the beads due to the force \mathbf{F}_μ is neglected. A bead-spring chain model incorporating bead inertia has shown that the neglect of bead inertia is justified in most practical situations [37]. The equation of motion is consequently obtained by setting $\mathbf{F}_\mu = \mathbf{o}$. Here, we consider the following force balance on each bead μ ,

$$\mathbf{F}_\mu^{(h)} + \mathbf{F}_\mu^{(b)} + \mathbf{F}_\mu^{(\phi)} + \mathbf{F}_\mu^{(iv)} = \mathbf{o} \quad (\mu = 1, 2, \dots, N) \quad (43)$$

where, $\mathbf{F}_\mu^{(h)}$ is the *hydrodynamic drag* force, $\mathbf{F}_\mu^{(b)}$ is the *Brownian* force, $\mathbf{F}_\mu^{(\phi)}$ is the *intramolecular* force due to the potential energy of the chain, and $\mathbf{F}_\mu^{(iv)}$ is the force due to the presence of *internal viscosity*. These are the various forces that have been considered so far in the literature, which are believed to play a crucial role in determining the polymer solution's transport properties. The nature of each of these forces is discussed in greater detail below. Note that, as is common in most theories, external forces acting on the bead have been neglected. However, their inclusion is reasonably straight forward [2].

The hydrodynamic drag force $\mathbf{F}_\mu^{(h)}$, is the force of resistance offered by the solvent to the motion of the bead μ . It is assumed to be proportional to the difference between the velocity-averaged bead velocity $\llbracket \dot{\mathbf{r}}_\mu \rrbracket$ and the local velocity of the solution,

$$\mathbf{F}_\mu^{(h)} = -\zeta [\llbracket \dot{\mathbf{r}}_\mu \rrbracket - (\mathbf{v}_\mu + \mathbf{v}'_\mu)] \quad (44)$$

where ζ is bead friction coefficient. Note that for spherical beads with radius a , in a solvent with viscosity η_s , the bead friction coefficient ζ is given by the Stokes expression: $\zeta = 6\pi\eta_s a$. The velocity-average of the bead velocity is not carried out with the Maxwellian distribution since this is just the mass-average solution velocity. However, it turns out that an explicit evaluation of the velocity-average is unnecessary for the development of the theory. Note that the velocity of the solution at bead μ has two components, the imposed flow field $\mathbf{v}_\mu = \mathbf{v}_0 + \boldsymbol{\kappa}(t) \cdot \mathbf{r}_\mu$, and the perturbation of the flow field \mathbf{v}'_μ due to the motion of the other beads of the chain. This perturbation is called *hydrodynamic interaction*, and its incorporation in molecular theories has proved to be of utmost importance in the prediction of transport properties. The presence of hydrodynamic interaction couples the motion of one bead in the chain to all the other beads, regardless of the distance between the beads along the length of the chain. In this sense, hydrodynamic interaction is a long range phenomena.

The perturbation to the flow field $\mathbf{v}'(\mathbf{r})$ at a point \mathbf{r} due to the presence of a point force $\mathbf{F}(\mathbf{r}')$ at the point \mathbf{r}' , can be found by solving the linearised Navier-Stokes equation [1, 8],

$$\mathbf{v}'(\mathbf{r}) = \boldsymbol{\Omega}(\mathbf{r} - \mathbf{r}') \cdot \mathbf{F}(\mathbf{r}') \quad (45)$$

where $\boldsymbol{\Omega}(\mathbf{r})$, called the *Oseen-Burgers tensor*, is the Green's function of the linearised Navier-Stokes equation,

$$\boldsymbol{\Omega}(\mathbf{r}) = \frac{1}{8\pi\eta_s r} \left(\mathbf{1} + \frac{\mathbf{r}\mathbf{r}}{r^2} \right) \quad (46)$$

The effect of hydrodynamic interaction is taken into account in polymer kinetic theory by treating the beads in the bead-spring chain as point particles. As a result, in response to the hydrodynamic drag force acting on each bead, each bead exerts an equal and opposite force on the solvent at the point that defines its location. The disturbance to the velocity at the bead ν is the sum of the disturbances caused by all the other beads in the chain, $\mathbf{v}'_\nu = -\sum_\mu \boldsymbol{\Omega}_{\nu\mu}(\mathbf{r}_\nu - \mathbf{r}_\mu) \cdot \mathbf{F}_\mu^{(h)}$, where, $\boldsymbol{\Omega}_{\mu\nu} = \boldsymbol{\Omega}_{\nu\mu}$ is given by,

$$\boldsymbol{\Omega}_{\mu\nu} = \begin{cases} \frac{1}{8\pi\eta_s r_{\mu\nu}} \left(\mathbf{1} + \frac{\mathbf{r}_{\mu\nu}\mathbf{r}_{\mu\nu}}{r_{\mu\nu}^2} \right), & \mathbf{r}_{\mu\nu} = \mathbf{r}_\mu - \mathbf{r}_\nu, \quad \text{for } \mu \neq \nu \\ 0 & \text{for } \mu = \nu \end{cases} \quad (47)$$

The Brownian force $\mathbf{F}_\mu^{(b)}$, on a bead μ is the result of the irregular collisions between the solvent molecules and the bead. Instead of representing the Brownian force by a randomly varying force, it is common in polymer kinetic theory to use an averaged Brownian force,

$$\mathbf{F}_\mu^{(b)} = -k_B T \left(\frac{\partial \ln \Psi}{\partial \mathbf{r}_\mu} \right) \quad (48)$$

As mentioned earlier, the origin of this expression can be understood within the framework of the complete phase space theory [2, 4]. Note that the Maxwellian distribution has been used to derive equation (48).

The total potential energy ϕ of the bead-spring chain is the sum of the potential energy S of the elastic springs, and the potential energy E due to the presence of excluded volume interactions between the beads. The force $\mathbf{F}_\mu^{(\phi)}$ on a bead μ due to the intramolecular potential energy ϕ is given by,

$$\mathbf{F}_\mu^{(\phi)} = -\frac{\partial \phi}{\partial \mathbf{r}_\mu} \quad (49)$$

In addition to the various forces discussed above, the *internal viscosity* force $\mathbf{F}_\mu^{(iv)}$, has received considerable attention in literature [3, 38, 43], though it appears not to have widespread acceptance. Various physical reasons have been cited as being responsible for the internal viscosity force. For instance, the hindrance to internal rotations due to the presence of energy barriers, the friction between two monomers on a chain that are close together in space and have a non-zero relative velocity, and so on. The simplest models for the internal viscosity force assume that it acts only between neighbouring beads in a bead-spring chain, and depends on the average relative velocities of these beads. Thus, for a bead μ that is not at the chain ends,

$$\mathbf{F}_\mu^{(iv)} = \varphi \left(\frac{(\mathbf{r}_{\mu+1} - \mathbf{r}_\mu)(\mathbf{r}_{\mu+1} - \mathbf{r}_\mu)}{|\mathbf{r}_{\mu+1} - \mathbf{r}_\mu|^2} \right) \cdot \llbracket \dot{\mathbf{r}}_{\mu+1} - \dot{\mathbf{r}}_\mu \rrbracket - \varphi \left(\frac{(\mathbf{r}_\mu - \mathbf{r}_{\mu-1})(\mathbf{r}_\mu - \mathbf{r}_{\mu-1})}{|\mathbf{r}_\mu - \mathbf{r}_{\mu-1}|^2} \right) \cdot \llbracket \dot{\mathbf{r}}_\mu - \dot{\mathbf{r}}_{\mu-1} \rrbracket \quad (50)$$

where φ is the internal viscosity coefficient. A scaling theory for a more general model that accounts for internal friction between arbitrary pairs of monomers has also been developed [35].

The equation of motion for bead ν can consequently be written as,

$$-\zeta \left[\llbracket \dot{\mathbf{r}}_\nu \rrbracket - \mathbf{v}_0 - \boldsymbol{\kappa} \cdot \mathbf{r}_\nu + \sum_\mu \boldsymbol{\Omega}_{\nu\mu} \cdot \mathbf{F}_\mu^{(h)} \right] - k_B T \frac{\partial \ln \Psi}{\partial \mathbf{r}_\nu} + \mathbf{F}_\nu^{(\phi)} + \mathbf{F}_\nu^{(iv)} = \mathbf{o} \quad (51)$$

Since $\mathbf{F}_\mu^{(h)} = k_B T (\partial \ln \Psi / \partial \mathbf{r}_\mu) - \mathbf{F}_\mu^{(\phi)} - \mathbf{F}_\mu^{(iv)}$, equation (51) can be rearranged to give,

$$\llbracket \dot{\mathbf{r}}_\nu \rrbracket = \mathbf{v}_0 + \boldsymbol{\kappa} \cdot \mathbf{r}_\nu + \frac{1}{\zeta} \sum_\mu \gamma_{\mu\nu} \cdot \left(-k_B T \frac{\partial \ln \Psi}{\partial \mathbf{r}_\mu} + \mathbf{F}_\mu^{(\phi)} + \mathbf{F}_\mu^{(iv)} \right) \quad (52)$$

where $\gamma_{\mu\nu}$ is the dimensionless *diffusion tensor* [2],

$$\gamma_{\mu\nu} = \delta_{\mu\nu} \mathbf{1} + \zeta \boldsymbol{\Omega}_{\nu\mu} \quad (53)$$

By manipulating equation (52), it is possible to rewrite the equation of motion in terms of the velocities of the center of mass \mathbf{r}_c and the bead-connector vectors \mathbf{Q}_k ,

$$\llbracket \dot{\mathbf{r}}_c \rrbracket = \mathbf{v}_0 + \boldsymbol{\kappa} \cdot \mathbf{r}_c - \frac{1}{N\zeta} \sum_{\nu,\mu,k} \bar{B}_{k\mu} \gamma_{\mu\nu} \cdot \left(k_B T \frac{\partial \ln \Psi}{\partial \mathbf{Q}_k} + \frac{\partial \phi}{\partial \mathbf{Q}_k} + \mathbf{f}_k^{(iv)} \right) \quad (54)$$

$$\llbracket \dot{\mathbf{Q}}_j \rrbracket = \boldsymbol{\kappa} \cdot \mathbf{Q}_j - \frac{1}{\zeta} \sum_k \tilde{A}_{jk} \cdot \left(k_B T \frac{\partial \ln \Psi}{\partial \mathbf{Q}_k} + \frac{\partial \phi}{\partial \mathbf{Q}_k} + \mathbf{f}_k^{(iv)} \right) \quad (55)$$

where, $\bar{B}_{k\nu}$ is defined by, $\bar{B}_{k\nu} = \delta_{k+1,\nu} - \delta_{k\nu}$, the internal viscosity force, $\mathbf{f}_k^{(iv)}$, in the direction of the connector vector \mathbf{Q}_k is,

$$\mathbf{f}_k^{(iv)} = \varphi \frac{\mathbf{Q}_k \mathbf{Q}_k}{|\mathbf{Q}_k|^2} \cdot \llbracket \dot{\mathbf{Q}}_k \rrbracket \quad (56)$$

and the tensor \tilde{A}_{jk} which accounts for the presence of hydrodynamic interaction is defined by,

$$\tilde{A}_{jk} = \sum_{\nu,\mu} \bar{B}_{j\nu} \gamma_{\mu\nu} \bar{B}_{k\mu} = A_{jk} \mathbf{1} + \zeta (\boldsymbol{\Omega}_{j,k} + \boldsymbol{\Omega}_{j+1,k+1} - \boldsymbol{\Omega}_{j,k+1} - \boldsymbol{\Omega}_{j+1,k}) \quad (57)$$

Here, A_{jk} is the Rouse matrix,

$$A_{jk} = \begin{cases} 2 & \text{for } |j-k| = 0, \\ -1 & \text{for } |j-k| = 1, \\ 0 & \text{otherwise} \end{cases} \quad (58)$$

In order to obtain the *diffusion* equation for a dilute solution of bead-spring chains, the equation of motion derived here must be combined with an equation of continuity.

3.2.3. The diffusion equation

The equation of continuity or ‘probability conservation’, which states that a bead-spring chain that disappears from one configuration must appear in another, has the form [2],

$$\frac{\partial \Psi}{\partial t} = - \sum_\nu \frac{\partial}{\partial \mathbf{r}_\nu} \cdot \llbracket \dot{\mathbf{r}}_\nu \rrbracket \Psi \quad (59)$$

The independence of Ψ from the location of the center of mass for homogeneous flows, and the result $\text{tr } \boldsymbol{\kappa} = 0$, for an incompressible fluid, can be shown to imply that the equation of continuity can be written in terms of internal coordinates alone as [2],

$$\frac{\partial \psi}{\partial t} = - \sum_j \frac{\partial}{\partial \mathbf{Q}_j} \cdot \llbracket \dot{\mathbf{Q}}_j \rrbracket \psi \quad (60)$$

The general diffusion equation which governs the time evolution of the instantaneous configurational distribution function ψ , in the presence of hydrodynamic interaction, arbitrary spring and excluded

volume forces, and an internal viscosity force given by equation (56), is obtained by substituting the equation of motion for $[\mathbf{Q}_j]$ from equation (55) into equation (60). It has the form,

$$\frac{\partial \psi}{\partial t} = - \sum_j \frac{\partial}{\partial \mathbf{Q}_j} \cdot \left(\boldsymbol{\kappa} \cdot \mathbf{Q}_j - \frac{1}{\zeta} \sum_k \tilde{\mathbf{A}}_{jk} \cdot \left[\frac{\partial \phi}{\partial \mathbf{Q}_k} + \mathbf{f}_k^{(iv)} \right] \right) \psi + \frac{k_B T}{\zeta} \sum_{j,k} \frac{\partial}{\partial \mathbf{Q}_j} \cdot \tilde{\mathbf{A}}_{jk} \cdot \frac{\partial \psi}{\partial \mathbf{Q}_k} \quad (61)$$

Equations such as (61) are also referred to as *Fokker-Planck* or *Smoluchowski* equations in the literature. The diffusion equation (61) is the most fundamental equation of the kinetic theory of dilute polymer solutions since a knowledge of ψ , for a flow field specified by $\boldsymbol{\kappa}$, would make it possible to evaluate averages of various configuration dependent quantities and thereby permit comparison of theoretical predictions with experimental observations.

The diffusion equation can be used to derive the time evolution equation of the average of any arbitrary configuration dependent quantity, $X(\mathbf{Q}_1, \dots, \mathbf{Q}_{N-1})$, by multiplying the left and right hand sides of equation (61) by X and integrating both sides over all possible configurations,

$$\frac{d\langle X \rangle}{dt} = \sum_j \langle \boldsymbol{\kappa} \cdot \mathbf{Q}_j \cdot \frac{\partial X}{\partial \mathbf{Q}_j} \rangle - \frac{k_B T}{\zeta} \sum_{j,k} \langle \tilde{\mathbf{A}}_{jk} \cdot \frac{\partial \ln \psi}{\partial \mathbf{Q}_k} \cdot \frac{\partial X}{\partial \mathbf{Q}_j} \rangle - \frac{1}{\zeta} \sum_{j,k} \langle \tilde{\mathbf{A}}_{jk} \cdot \left[\frac{\partial \phi}{\partial \mathbf{Q}_k} + \mathbf{f}_k^{(iv)} \right] \cdot \frac{\partial X}{\partial \mathbf{Q}_j} \rangle \quad (62)$$

Except for a situation where nearly all the important microscopic phenomena are neglected, the diffusion equation (61) is unfortunately in general analytically insoluble. There have been very few attempts to directly solve diffusion equations with the help of a numerical solution procedure [9, 10]. In this context it is worth bearing in mind that what are usually required are averages of configuration dependent quantities. However, in general even averages cannot be obtained exactly by solving equation (62). As a result, it is common in most molecular theories to obtain the averages by means of various approximations.

In order to examine the validity of these approximations it is vitally important to compare the approximate predictions of transport properties with the exact predictions of the models. One of the ways by which exact numerical results may be obtained is by adopting a numerical procedure based on the mathematical equivalence of diffusion equations in polymer configuration space and stochastic differential equations for the polymer configuration [29]. Instead of numerically solving the analytically intractable diffusion equation for the distribution function, stochastic trajectories can be generated by *Brownian dynamics simulations* based on a numerical integration of the appropriate stochastic differential equation. Averages calculated from stochastic trajectories (obtained as a solution of the stochastic differential equations), are identical to the averages calculated from distribution functions (obtained as a solution of the diffusion equations). It has now become fairly common for any new approximate molecular theory of a microscopic phenomenon to establish the accuracy of the results with the help of Brownian dynamics simulations. In this chapter, while results of such simulations are cited, details of the development of the appropriate stochastic differential equations are not discussed. A comprehensive introduction to the development of stochastic differential equations which are equivalent to given diffusion equations for the probability density in configuration space, can be found in the treatise by Öttinger [29].

3.2.4. The stress tensor

The expression for the stress tensor in a dilute polymer solution was originally obtained by the use of simple physical arguments which considered the various mechanisms that contributed to the flux of momentum across an oriented surface in the fluid [2]. The major mechanisms considered were the transport of momentum by beads crossing the surface, and the tension in the springs that straddle the surface. These physical arguments help to provide an intuitive understanding of the origin of the different terms in the stress tensor expression. On the other hand, such arguments are difficult to pursue in the presence of complicated microscopic phenomena, and there is uncertainty about the completeness of the final expression. An alternative approach to the derivation of the expression for the stress tensor has been to use more fundamental arguments that consider the complete phase space of the polymeric fluid [2, 4].

A very general expression for the polymer contribution to the stress tensor, derived by adopting the complete phase space approach, for models without constraints such as the bead-spring chain model, in the presence of hydrodynamic interaction and an arbitrary intramolecular potential force, is the *modified Kramers* expression [2],

$$\boldsymbol{\tau}^p = n_p \sum_{\nu} \langle (\mathbf{r}_{\nu} - \mathbf{r}_c) \mathbf{F}_{\nu}^{(\phi)} \rangle + (N - 1) n_p k_B T \mathbf{1} \quad (63)$$

When rewritten in terms of the internal coordinates of a bead-spring chain, equation (63) assumes a form called the *Kramers* expression,

$$\boldsymbol{\tau}^p = -n_p \sum_j \langle \mathbf{Q}_j \frac{\partial \phi}{\partial \mathbf{Q}_j} \rangle + (N - 1) n_p k_B T \mathbf{1} \quad (64)$$

It is important to note that the presence of internal viscosity has not been taken into account in the phase space theories used to derive the modified Kramers expression (63). When examined from the standpoint of thermodynamic considerations, the proper form of the stress tensor in the presence of internal viscosity appears to be the Giesekus expression rather than the Kramers expression [39]. Since predictions of models with internal viscosity are not considered in this chapter, the Giesekus expression is not discussed here.

In order to evaluate the stress tensor, for various choices of the potential energy ϕ , it turns out that it is usually necessary to evaluate the second moments of the bead connector vectors, $\langle \mathbf{Q}_j \mathbf{Q}_k \rangle$. An equation that governs the time evolution of the second moments can be obtained with the help of equation (62). It has the form,

$$\begin{aligned} \frac{d}{dt} \langle \mathbf{Q}_j \mathbf{Q}_k \rangle &= \boldsymbol{\kappa} \cdot \langle \mathbf{Q}_j \mathbf{Q}_k \rangle + \langle \mathbf{Q}_j \mathbf{Q}_k \rangle \cdot \boldsymbol{\kappa}^{\dagger} + \frac{2k_B T}{\zeta} \langle \tilde{\mathbf{A}}_{jk} \rangle \\ &- \frac{1}{\zeta} \sum_m \left\{ \langle \mathbf{Q}_j \left[\frac{\partial \phi}{\partial \mathbf{Q}_m} + \mathbf{f}_m^{(iv)} \right] \cdot \tilde{\mathbf{A}}_{mk} \rangle + \langle \tilde{\mathbf{A}}_{jm} \cdot \left[\frac{\partial \phi}{\partial \mathbf{Q}_m} + \mathbf{f}_m^{(iv)} \right] \cdot \mathbf{Q}_k \rangle \right\} \end{aligned} \quad (65)$$

The second moment equation (65), which is an ordinary differential equation, is in general not a closed equation for $\langle \mathbf{Q}_j \mathbf{Q}_k \rangle$, since it involves higher order moments on the right hand side.

Within the context of the molecular theory developed thus far, it is clear that the prediction of the rheological properties of dilute polymer solutions with a bead-spring chain model usually requires the solution of the second moment equation (65). To date however, there are no solutions to the general second moment equation (65) which simultaneously incorporates the microscopic phenomena of hydrodynamic interaction, excluded volume, non-linear spring forces and internal viscosity. Attempts have so far been restricted to treating a smaller set of combinations of these phenomenon. The simplest molecular theory, based on a bead-spring chain model, for the prediction of the transport properties of dilute polymer solutions is the Rouse model. The Rouse model neglects all the microscopic phenomenon listed above, and consequently fails to predict many of the observed features of dilute solution behavior. In a certain sense, however, it provides the framework and motivation for all further improvements in the molecular theory. The Rouse model and its predictions are introduced below, while improvements in the treatment of hydrodynamic interactions alone are discussed subsequently.

3.3. The Rouse model

The Rouse model assumes that the springs of the bead-spring chain are governed by a Hookean spring force law. The only solvent-polymer interactions treated are that of hydrodynamic drag and Brownian bombardment. The diffusion equation (61) with the effects of hydrodynamic interaction, excluded volume and internal viscosity neglected, and with a Hookean spring force law, has the form,

$$\frac{\partial \psi}{\partial t} = - \sum_j \frac{\partial}{\partial \mathbf{Q}_j} \cdot \left(\boldsymbol{\kappa} \cdot \mathbf{Q}_j - \frac{H}{\zeta} \sum_k A_{jk} \mathbf{Q}_k \right) \psi + \frac{k_B T}{\zeta} \sum_{j,k} A_{jk} \frac{\partial}{\partial \mathbf{Q}_j} \cdot \frac{\partial \psi}{\partial \mathbf{Q}_k} \quad (66)$$

The diffusion equation (66) has an analytical solution since it is linear in the bead-connector vectors. It is satisfied by a Gaussian distribution,

$$\psi(\mathbf{Q}_1, \dots, \mathbf{Q}_{N-1}) = \mathcal{N}(t) \exp \left[-\frac{1}{2} \sum_{j,k} \mathbf{Q}_j \cdot (\boldsymbol{\sigma}^{-1})_{jk} \cdot \mathbf{Q}_k \right] \quad (67)$$

where $\mathcal{N}(t)$ is the normalisation factor, and the tensor $\boldsymbol{\sigma}_{jk}$ which uniquely characterises the Gaussian distribution is identical to the second moment,

$$\boldsymbol{\sigma}_{jk} \equiv \langle \mathbf{Q}_j \mathbf{Q}_k \rangle \quad (68)$$

Note that the tensors $\boldsymbol{\sigma}_{jk}$ are not symmetric, but satisfy the relation $\boldsymbol{\sigma}_{jk} = \boldsymbol{\sigma}_{kj}^T$. (Further information on linear diffusion equations and Gaussian distributions can be obtained in the extended discussion in Appendix A of [22]).

Since the intramolecular potential in the Rouse model is only due to the presence of Hookean springs, it is straight forward to see that the Kramers expression for the stress tensor $\boldsymbol{\tau}^p$, is given by,

$$\boldsymbol{\tau}^p = -n_p H \sum_j \boldsymbol{\sigma}_{jj} + (N-1) n_p k_B T \mathbf{1} \quad (69)$$

The tensors $\boldsymbol{\sigma}_{jj}$ are obtained by solving the second moment equation (65), which becomes a closed equation for the second moments when the Rouse assumptions are made. It has the form,

$$\frac{d}{dt} \boldsymbol{\sigma}_{jk} - \boldsymbol{\kappa} \cdot \boldsymbol{\sigma}_{jk} - \boldsymbol{\sigma}_{jk} \cdot \boldsymbol{\kappa}^\dagger = \frac{2k_B T}{\zeta} A_{jk} \mathbf{1} - \frac{H}{\zeta} \sum_m [\boldsymbol{\sigma}_{jm} A_{mk} + A_{jm} \boldsymbol{\sigma}_{mk}] \quad (70)$$

Note that the solution of equation (70) also leads to the complete specification of the Gaussian configurational distribution function ψ .

A *Hookean dumbbell* model, which is the simplest example of a bead-spring chain, is obtained by setting $N = 2$. It is often used for preliminary calculations since its simplicity makes it possible to obtain analytical solutions where numerical solutions are unavoidable for longer chains. For such a model, substituting for $\boldsymbol{\sigma}_{11}$ in terms of $\boldsymbol{\tau}^p$ from equation (69) into equation (70), leads to following equation for the polymer contribution to the stress tensor,

$$\boldsymbol{\tau}^p + \lambda_H \boldsymbol{\tau}_{(1)}^p = -n_p k_B T \lambda_H \dot{\boldsymbol{\gamma}} \quad (71)$$

where $\boldsymbol{\tau}_{(1)}^p = d\boldsymbol{\tau}^p/dt - \boldsymbol{\kappa} \cdot \boldsymbol{\tau}^p - \boldsymbol{\tau}^p \cdot \boldsymbol{\kappa}^\dagger$, is the convected time derivative [2] of $\boldsymbol{\tau}^p$, and $\lambda_H = (\zeta/4H)$ is a time constant. Equation (71) indicates that a Hookean dumbbell model with the Rouse assumptions leads to a convected Jeffreys model or Oldroyd-B model as the constitutive equation for a dilute polymer solution. This is perhaps the simplest coarse-grained microscopic model capable of reproducing some of the macroscopic rheological properties of dilute polymer solutions.

In the case of a bead-spring chain with $N > 2$, it is possible to obtain a similar insight into the nature of the stress tensor by introducing *normal coordinates*. These coordinates help to decouple the connector vectors $\mathbf{Q}_1, \dots, \mathbf{Q}_{N-1}$, which are coupled to each other because of the Rouse matrix.

The connector vectors are mapped to a new set of normal coordinates, $\mathbf{Q}'_1, \dots, \mathbf{Q}'_{N-1}$ with the transformation,

$$\mathbf{Q}_j = \sum_k \Pi_{jk} \mathbf{Q}'_k \quad (72)$$

where, Π_{jk} are the elements of an orthogonal matrix with the property

$$(\Pi^{-1})_{jk} = \Pi_{kj}, \text{ such that, } \sum_m \Pi_{mj} \Pi_{mk} = \delta_{jk} \quad (73)$$

The orthogonal matrix Π_{jk} , which will henceforth be referred to as the Rouse orthogonal matrix, diagonalises the Rouse matrix A_{jk} ,

$$\sum_{j,k} \Pi_{ji} A_{jk} \Pi_{kl} = a_l \delta_{il} \quad (74)$$

where, the Rouse eigenvalues a_l are given by $a_l = 4 \sin^2(l\pi/2N)$. The elements of the Rouse orthogonal matrix are given by the expression,

$$\Pi_{jk} = \sqrt{\frac{2}{N}} \sin\left(\frac{jk\pi}{N}\right) \quad (75)$$

The diffusion equation in terms of these normal coordinates, admits a solution for the configurational distribution function of the form [2]

$$\psi(\mathbf{Q}'_1, \dots, \mathbf{Q}'_{N-1}) = \prod_{k=1}^{N-1} \psi_k(\mathbf{Q}'_k) \quad (76)$$

As a consequence, the diffusion equation becomes uncoupled and can be simplified to $(N - 1)$ diffusion equations, one for each of the $\psi_k(\mathbf{Q}'_k)$. Since the \mathbf{Q}'_k are independent of each other, all the covariances $\langle \mathbf{Q}'_j \mathbf{Q}'_k \rangle$ with $j \neq k$ are zero, and only the $(N - 1)$ variances $\sigma'_j \equiv \langle \mathbf{Q}'_j \mathbf{Q}'_j \rangle$ are non-zero. Evolution equations for the variances σ'_j can then be derived from these uncoupled diffusion equations with the help of a procedure similar to that used for the derivation of equation (65).

The stress tensor is given in terms of σ'_j by the expression,

$$\boldsymbol{\tau}^p = \sum_j \boldsymbol{\tau}_j^p \quad (77)$$

where,

$$\boldsymbol{\tau}_j^p = -n_p H \sigma'_j + n_p k_B T \mathbf{1} \quad (78)$$

On substituting for σ'_j in terms of $\boldsymbol{\tau}_j^p$ from equation (78) into the evolution equation for σ'_j , one obtains,

$$\boldsymbol{\tau}_j^p + \lambda_j \boldsymbol{\tau}_{j(1)}^p = -n_p k_B T \lambda_j \dot{\boldsymbol{\gamma}} \quad (79)$$

where, the relaxation times λ_j are given by $\lambda_j = (\zeta/2H a_j)$. Consequently, each of the $\boldsymbol{\tau}_j^p$ satisfy an equation identical to equation (71) for the polymer contribution to the stress tensor in a Hookean dumbbell model. The Rouse model, therefore, leads to a constitutive equation that is a multimode generalization of the convected Jeffreys or Oldroyd B model.

It is clear from above discussion that the process of transforming to normal coordinates enables one to derive a closed form expression for the stress tensor, and to gain the insight that the Rouse chain with N beads has N independent relaxation times which describe the different relaxation processes in the chain, from the entire chain to successively smaller sub-chains. It is straight forward to show that for large N , the longest relaxation times λ_j scale with chain length as N^2 .

A few important transport property predictions which show the limitations of the Rouse model are considered briefly below. It is worth noting that since the Rouse model does not include the effect of excluded volume, its predictions are restricted to dilute solutions of polymers in theta solvents. This restriction is infact applicable to all the models of hydrodynamic interaction treated here.

In steady simple shear flow, with $\boldsymbol{\kappa}(t)$ given by equation (4), the three independent material functions that characterise such flows are [2],

$$\eta_p = n_p k_B T \sum_j \lambda_j; \quad \Psi_1 = 2n_p k_B T \sum_j \lambda_j^2; \quad \Psi_2 = 0 \quad (80)$$

It is clear that the Rouse model accounts for the presence of viscoelasticity through the prediction of a nonzero first normal stress difference in simple shear flow. However, it does not predict the nonvanishing of the second normal stress difference, and the shear rate dependence of the viscometric functions.

From the definition of intrinsic viscosity (1) and the fact that $\rho_p \sim N n_p$, it follows from equation (80) that for the Rouse model, $[\eta]_0 \sim N$. This is at variance with the experimental results discussed earlier, and displayed in equation (11). It is also straight forward to see that the Rouse model predicts that the characteristic relaxation time scales as the square of the chain length, $\lambda_p \sim N^2$.

In small amplitude oscillatory shear, $\kappa(t)$ is given by equation (6), and expressions for the material functions G' and G'' in terms of the relaxation times λ_j can be easily obtained [2]. In the intermediate frequency range, where as discussed earlier, experimental results indicate that both G' and G'' scale as $\omega^{2/3}$, the Rouse model predicts a scaling $\omega^{1/2}$ [17].

The translational diffusion coefficient D for a bead-spring chain at equilibrium can be obtained by finding the average friction coefficient Z for the entire chain in a quiescent solution, and subsequently using the Nernst-Einstein equation, $D = k_B T Z^{-1}$ [2]. It can be shown that for the Rouse model $Z = \zeta N$, *ie.* the total friction coefficient of the chain is a sum of the individual bead friction coefficients. As a result, the Rouse model predicts that the diffusion coefficient scales as the inverse of the molecular weight. This is not observed in dilute solutions. Instead experiments indicate the scaling depicted in equation (12).

The serious shortcomings of the Rouse model highlighted above have been the motivation for the development of more refined molecular theories. The scope of this chapter is restricted to reviewing recent advances in the treatment of hydrodynamic interaction.

4. HYDRODYNAMIC INTERACTION

Hydrodynamic interaction, as pointed out earlier, is a long range interaction between the beads which arises because of the solvent's capacity to propagate one bead's motion to another through perturbations in its velocity field. It was first introduced into framework of polymer kinetic theory by Kirkwood and Riseman [14]. As we have seen in the development of the general diffusion equation above, it is reasonably straight forward to include hydrodynamic interaction into the framework of the molecular theory. However, it renders the resultant equations analytically intractable and as a result, various attempts have been made in order to solve them approximately.

In this section, we review the various approximation schemes introduced over the years. The primary test of an approximate model is of course its capacity to predict experimental observations. The accuracy of the approximation however, can only be assessed by checking the proximity of the approximate results to the exact numerical results obtained by Brownian dynamics simulations. Finally, the usefulness of an approximation depends on its computational intensity. The individual features and deficiencies of the different approximations will be examined in the light of these observations.

In the presence of hydrodynamic interaction, and with excluded volume and internal viscosity neglected, a bead-spring chain with Hookean springs has a configurational distribution function ψ that must satisfy the following simplified form of the diffusion equation (61),

$$\frac{\partial \psi}{\partial t} = - \sum_j \frac{\partial}{\partial \mathbf{Q}_j} \cdot \left(\boldsymbol{\kappa} \cdot \mathbf{Q}_j - \frac{H}{\zeta} \sum_k \tilde{\mathbf{A}}_{jk} \cdot \mathbf{Q}_k \right) \psi + \frac{k_B T}{\zeta} \sum_{j,k} \frac{\partial}{\partial \mathbf{Q}_j} \cdot \tilde{\mathbf{A}}_{jk} \cdot \frac{\partial \psi}{\partial \mathbf{Q}_k} \quad (81)$$

while the second moment equation (65) assumes the form,

$$\frac{d}{dt} \langle \mathbf{Q}_j \mathbf{Q}_k \rangle = \boldsymbol{\kappa} \cdot \langle \mathbf{Q}_j \mathbf{Q}_k \rangle + \langle \mathbf{Q}_j \mathbf{Q}_k \rangle \cdot \boldsymbol{\kappa}^\dagger + \frac{2k_B T}{\zeta} \langle \tilde{\mathbf{A}}_{jk} \rangle - \frac{H}{\zeta} \sum_m \left[\langle \mathbf{Q}_j \mathbf{Q}_m \cdot \tilde{\mathbf{A}}_{mk} \rangle + \langle \tilde{\mathbf{A}}_{jm} \cdot \mathbf{Q}_m \mathbf{Q}_k \rangle \right] \quad (82)$$

Equation (82) is not a closed equation for the second moments since it involves more complicated moments on the right hand side. This is the central problem of all molecular theories which attempt to

predict the rheological properties of dilute polymer solutions and that incorporate hydrodynamic interaction. The different approximate treatments of hydrodynamic interaction, which are discussed roughly chronologically below, basically reduce to finding a suitable closure approximation for the second moment equation.

4.1. The Zimm model

The Zimm model was the first attempt at improving the Rouse model by introducing the effect of hydrodynamic interaction in a preaveraged or equilibrium-averaged form. The preaveraging approximation has been very frequently used in polymer literature since its introduction by Kirkwood and Riseman [14]. The approximation consists of evaluating the average of the hydrodynamic tensor with the equilibrium distribution function (34), and replacing the hydrodynamic interaction tensor $\tilde{\mathbf{A}}_{jk}$, wherever it occurs in the governing equations, with its equilibrium average \tilde{A}_{jk} . (Note that the incorporation of the effect of hydrodynamic interaction does not alter the equilibrium distribution function, which is still given by (34) for bead-spring chains with Hookean springs.) The matrix \tilde{A}_{jk} is called the modified Rouse matrix, and is given by,

$$\tilde{A}_{jk} = A_{jk} + \sqrt{2} h^* \left(\frac{2}{\sqrt{|j-k|}} - \frac{1}{\sqrt{|j-k-1|}} - \frac{1}{\sqrt{|j-k+1|}} \right) \quad (83)$$

where, $h^* = a\sqrt{(H/\pi k_B T)}$ is the hydrodynamic interaction parameter. The hydrodynamic interaction parameter is approximately equal to the ratio of the bead radius to the equilibrium root mean square length of a single spring of the bead-spring chain. This implies that $h^* < 0.5$, since the beads cannot overlap. Typical values used for h^* are in the range $0.1 \leq h^* \leq 0.3$ [22].

By including the hydrodynamic interaction in an averaged form, the diffusion equation remains linear in the connector vectors, and consequently is satisfied by a Gaussian distribution (67) as in the Rouse case. However, the covariance tensors σ_{jk} are now governed by the set of differential equations (70) with the Rouse matrix A_{jk} replaced with the modified Rouse matrix \tilde{A}_{jk} . Note that this modified second moment equation is also a closed set of equations for the second moments.

As in the Rouse case, it is possible to simplify the solution of the Zimm model by carrying out a diagonalisation procedure. This is achieved by mapping the connector vectors to normal coordinates, as in (72), but in this case the Zimm orthogonal matrix Π_{jk} , which diagonalises the modified Rouse matrix,

$$\sum_{j,k} \Pi_{ji} \tilde{A}_{jk} \Pi_{kl} = \tilde{a}_l \delta_{il} \quad (84)$$

must be found numerically for $N > 4$. Here, \tilde{a}_l are the so called Zimm eigenvalues. The result of this procedure is to render the diffusion equation solvable by the method of separation of variables. Thus, as in the Rouse case, only the $(N-1)$ transformed coordinate variances σ_j^p are non-zero, and differential equations governing these variances can be derived by manipulating the uncoupled diffusion equations.

The diagonalisation procedure enables the polymer contribution to the stress tensor τ^p in the Zimm model to be expressed as a sum of partial stresses τ_j^p as in equation (77), but the τ_j^p now satisfy equation (79) with the ‘Rouse’ relaxation times λ_j replaced with ‘Zimm’ relaxation times $\tilde{\lambda}_j$. The Zimm relaxation times are defined by $\tilde{\lambda}_j = (\zeta/2H \tilde{a}_j)$.

From the discussion above, it is clear that the Zimm model differs from the Rouse model only in the spectrum of relaxation times. As we shall see shortly, this leads to a significant improvement in the prediction of linear viscoelastic properties and the scaling of transport properties with molecular weight in theta solvents. The Zimm model therefore establishes unequivocally the importance of the microscopic phenomenon of hydrodynamic interaction. On the other hand, it does not lead to any improvement in the prediction of nonlinear properties, and consequently subsequent treatments of hydrodynamic interaction have concentrated on improving this aspect of the Zimm model.

By considering the long chain limit of the Zimm model, *ie.*, $N \rightarrow \infty$, it is possible to discuss the universal properties predicted by the model. The various power law dependences of transport properties on molecular weight, characterised by universal exponents, and universal ratios formed from the prefactors of these dependences can be obtained. These predictions are ideal for comparison with experimental data on high molecular weight polymer solutions since they are parameter free. We shall discuss some universal exponents predicted by the Zimm model below, while universal ratios are discussed later in the chapter.

As mentioned above, the first noticeable change upon the introduction of hydrodynamic interaction is the change in the relaxation spectrum. In the long chain limit, the longest relaxation times $\tilde{\lambda}_j$ scale with chain length as $N^{3/2}$ [29], whereas we had found earlier that the chain length dependence of the longest relaxation times in the Rouse model was N^2 .

In steady simple shear flow, the Zimm model like the Rouse model, fails to predict the experimentally observed occurrence of non-zero second normal stress differences and the experimentally observed shear rate dependence of the viscometric functions. It does however lead to an improved prediction of the scaling of the zero shear rate intrinsic viscosity with molecular weight, $[\eta]_0 \sim N^{1/2}$. This prediction is in agreement with experimental results for the Mark-Houwink exponent in theta solvents (see equation (11)). As with the longest relaxation times, the characteristic relaxation time $\lambda_p \sim N^{3/2}$.

In small amplitude oscillatory shear, the Zimm model predicts that the material functions G' and G'' scale with frequency as $\omega^{2/3}$ in the intermediate frequency range. This is in exceedingly good agreement with experimental results [2, 17].

The translational diffusion coefficient D for chainlike molecules at equilibrium, with preaveraged hydrodynamic interaction, was originally obtained by Kirkwood [14]. Subsequently, several workers obtained a correction to the Kirkwood diffusion coefficient for the Zimm model [21]. The exact results differ by less than 2% from the Kirkwood value for all values of the chain length and h^* . Interestingly, three different approaches to obtaining the diffusion coefficient, namely, the Nernst-Einstein equation, the calculation of the mean-square displacement caused by Brownian forces, and the study of the time evolution of concentration gradients, lead to identical expressions for the diffusion coefficient [21]. In the limit of very long chains, it can be shown that $D \sim N^{-1/2}$. The Zimm model therefore gives the correct dependence of translational diffusivity on molecular weight in theta solvents.

The Zimm result for the translational diffusivity has been traditionally interpreted to mean that the polymer coil in a theta solvent behaves like a rigid sphere, with radius equal to the root mean square end-to-end distance. This follows from the fact that the diffusion coefficient for a rigid sphere scales as the inverse of the radius of the sphere, and in a theta solvent, $\langle r^2 \rangle_{\text{eq}}$ scales with chain length as N . The solvent inside the coil is believed to be dragged along with the coil, and the inner most beads of the bead-spring chain are considered to be shielded from the velocity field due to the presence of hydrodynamic interaction [44, 17]. This intuitive notion has been used to point out the difference between the Zimm and the Rouse model, where all the N beads of the polymer chain are considered to be exposed to the applied velocity field. Recently, by explicitly calculating the velocity field inside a polymer coil in the Zimm model, Öttinger [30] has shown that the solvent motion inside a polymer coil is different from that of a rigid sphere throughout the polymer coil, and that shielding from the velocity field occurs only to a certain extent.

4.2. The consistent averaging approximation

The first predictions of shear thinning were obtained when hydrodynamic interaction was treated in a more precise manner than that of preaveraging the hydrodynamic interaction tensor. In order to make the diffusion equation (81) linear in the connector vectors, as pointed out earlier, it is necessary to average the hydrodynamic interaction tensor. However, it is not necessary to preaverage the hydrodynamic interaction tensor with the equilibrium distribution. On the other hand, the average can be carried out with the non-equilibrium distribution function (67). The linearity of the diffusion equation ensures that its solution is a Gaussian distribution. Öttinger [20, 22] suggested that the hydrodynamic interaction tensor occurring in the diffusion equation be replaced with its non-equilibrium average. Since it is necessary to know the averaged hydrodynamic interaction tensor in order to find the non-equilibrium distribution function,

both the averaged hydrodynamic interaction tensor and the non-equilibrium distribution function must be obtained in a *self-consistent* manner.

Several years ago, Fixman [11] introduced an iterative scheme (beginning with the equilibrium distribution function), for refining the distribution function with which to carry out the average of the hydrodynamic interaction tensor. The self-consistent scheme of Öttinger is recovered if the iterative procedure is repeated an infinite number of times. However, Fixman carried out the iteration only upto one order higher than the preaveraging stage.

The average of the hydrodynamic interaction tensor evaluated with the Gaussian distribution (67) is an $(N - 1) \times (N - 1)$ matrix with tensor components, $\overline{\mathbf{A}}_{jk}$, defined by,

$$\overline{\mathbf{A}}_{jk} = A_{jk} \mathbf{1} + \sqrt{2}h^* \left[\frac{\mathbf{H}(\hat{\boldsymbol{\sigma}}_{j,k})}{\sqrt{|j-k|}} + \frac{\mathbf{H}(\hat{\boldsymbol{\sigma}}_{j+1,k+1})}{\sqrt{|j-k|}} - \frac{\mathbf{H}(\hat{\boldsymbol{\sigma}}_{j,k+1})}{\sqrt{|j-k-1|}} - \frac{\mathbf{H}(\hat{\boldsymbol{\sigma}}_{j+1,k})}{\sqrt{|j-k+1|}} \right] \quad (85)$$

where the tensors $\hat{\boldsymbol{\sigma}}_{\mu\nu}$ are given by,

$$\hat{\boldsymbol{\sigma}}_{\mu\nu} = \hat{\boldsymbol{\sigma}}_{\mu\nu}^\dagger = \hat{\boldsymbol{\sigma}}_{\nu\mu} = \frac{1}{|\mu - \nu|} \frac{H}{k_B T} \sum_{j,k=\min(\mu,\nu)}^{\max(\mu,\nu)-1} \boldsymbol{\sigma}_{jk} \quad (86)$$

and the function of the second moments, $\mathbf{H}(\boldsymbol{\sigma})$ is,

$$\mathbf{H}(\boldsymbol{\sigma}) = \frac{3}{2(2\pi)^{3/2}} \int d\mathbf{k} \frac{1}{k^2} \left(\mathbf{1} - \frac{\mathbf{k}\mathbf{k}}{k^2} \right) \exp\left(-\frac{1}{2}\mathbf{k} \cdot \boldsymbol{\sigma} \cdot \mathbf{k}\right) \quad (87)$$

Note that the convention $\mathbf{H}(\hat{\boldsymbol{\sigma}}_{jj})/0 = 0$ has been adopted in equation (85) above.

The self-consistent closure approximation therefore consists of replacing the hydrodynamic interaction tensor $\tilde{\mathbf{A}}_{jk}$ in equation (82) with its non-equilibrium average $\overline{\mathbf{A}}_{jk}$. As in the earlier approximations, this leads to a system of $(N - 1)^2$ coupled ordinary differential equations for the components of the covariance matrix $\boldsymbol{\sigma}_{jk}$. Their solution permits the evaluation of the stress tensor through the Kramers expression (69), and as a consequence all the relevant material functions.

Viscometric functions in steady simple shear flows were obtained by Öttinger [20] for chains with $N \leq 25$ beads, while material functions in start-up of steady shear flow, cessation of steady shear flow, and stress relaxation after step-strain were obtained by Wedgewood and Öttinger [41] for chains with $N \leq 15$ beads. The latter authors also include consistently-averaged FENE springs in their model.

Shear rate dependent viscometric functions, and a nonzero *positive* second normal stress difference are predicted by the self-consistent averaging approximation; a marked improvement over the predictions of the Zimm model. Both the reduced viscosity and the reduced first normal stress difference initially decrease with increasing shear rate. However, for long enough chains, they begin to rise monotonically at higher values of the reduced shear rate β . This rise is a consequence of the weakening of hydrodynamic interaction in strong flows due to an increase in the separation between the beads of the chain. With increasing shear rate, the material functions tend to the shear rate independent Rouse values, which (for long enough chains), are higher than the zero shear rate consistently-averaged values. The prediction of shear thickening behavior is not in agreement with the shear thinning that is commonly observed experimentally. However, as mentioned earlier, some experiments with very high molecular weight systems seem to suggest the existence of shear thinning followed by shear thickening followed again by shear thinning as the shear rate is increased. While only shear thickening at high shear rates is predicted with Hookean springs, the inclusion of consistently-averaged FENE springs in the model leads to predictions which are qualitatively in agreement with these observations, with the FENE force becoming responsible for the shear thinning at very high shear rates [41, 15].

The means of examining the accuracy of various approximate treatments of hydrodynamic interaction was established when the problem was solved exactly with the help of Brownian dynamics simulations with full hydrodynamic interaction included [46, 48]. These simulations reveal that while the predictions

of the shear rate dependence of the viscosity and first normal stress difference by the self-consistent averaging procedure are in qualitative agreement with the Brownian dynamics simulations, they do not agree quantitatively. Further, in contrast to the consistent-averaging prediction, at low shear rates, a negative value for the second normal stress difference is obtained. As noted earlier, the sign of the second normal stress difference has not been conclusively established [3].

The computational intensity of the consistent-averaging approximation leads to an upper bound on the length of chain that can be examined. As a result, it is not possible to discuss the universal shear rate dependence of the viscometric functions predicted by it. On the other hand, it is possible to come to certain general conclusions regarding the nature of the stress tensor in the long chain limit, and to predict the zero shear rate limit of certain universal ratios [20]. Thus, it is possible to show the important result that the polymer contribution to the stress tensor depends only on a length scale and a time scale, and not on the strength of the hydrodynamic interaction parameter h^* . In the long chain limit, h^* can be absorbed into the basic time constant, and it does not occur in any of the non-dimensional ratios. Indeed this is also true of the finite extensibility parameter b , which can also be shown to have no influence on the long chain rheological properties [22]. The long chain limit of the consistent-averaging approximation is therefore a parameter free model.

It is possible to obtain an explicit representation of the modified Kramers matrix for infinitely long chains by introducing continuous variables in place of discrete indices [20]. This enables the analytical calculation of various universal ratios predicted by the consistent-averaging approximation. These predictions are discussed later in this chapter. However, two results are worth highlighting here. Firstly, it can be shown explicitly that the leading order corrections to the large N limit of the various universal ratios are of order $(1/\sqrt{N})$, and secondly, there is a special value of $h^* = 0.2424\dots$, at which the leading order corrections are of order $(1/N)$. These results have proven to be very useful for subsequent numerical exploration of the long chain limit in more accurate models of the hydrodynamic interaction.

Short chains with consistently-averaged hydrodynamic interaction, as noted earlier, do not show shear thickening behavior; this aspect is revealed only with increasing chain length. Furthermore, it is not clear with the kind of chain lengths that can be examined, whether the minimum in the viscosity and first normal stress curves continue to exist in the long chain limit [20]. The examination of long chain behavior is therefore important since aspects of polymer solution behavior might be revealed that are otherwise hidden when only short chains are considered. The introduction of the *decoupling approximation* by Magda, Larson and Mackay [18] and Kishbaugh and McHugh [15] made the examination of the shear rate dependence of long chains feasible. The decoupling approximation retains the accuracy of the self-consistent averaging procedure, but is much more computationally efficient.

4.3. The decoupling approximation

The decoupling approximation introduced by Magda *et al.* [18] and Kishbaugh and McHugh [15] (who use FENE springs in place of the Hookean springs of Magda *et al.*) consists of extending the ‘diagonalise and decouple’ procedure of the Rouse and Zimm theories to the case of the self consistently averaged theory. They first transform the connector vectors \mathbf{Q}_j to a new set of coordinates \mathbf{Q}'_j using the time-invariant Rouse orthogonal matrix Π_{jk} . (Kishbaugh and McHugh also use the Zimm orthogonal matrix). The same orthogonal matrix Π_{jk} is then assumed to diagonalise the matrix of *tensor* components $\bar{\mathbf{A}}_{jk}$. While the process of diagonalisation was exact in the Rouse and Zimm theories, it is an approximation in the case of the decoupling approximation. It implies that even in the self consistently averaged theory the diffusion equation can be solved by the method of separation of variables, and only the $(N - 1)$ transformed coordinate variances σ'_j are non-zero. The differential equations governing these variances can be derived from the uncoupled diffusion equations and solved numerically. The appropriate material functions are then obtained using the Kramers expression in terms of the transformed coordinates, namely, equations (77) and (78).

The decrease in the number of differential equations to be solved, from $(N - 1)^2$ for the covariances σ_{jk} to $(N - 1)$ for the variances σ'_j , is suggested by Kishbaugh and McHugh as the reason for the great reduction in computational time achieved by the decoupling approximation. Prakash and Öttinger [33]

discuss the reasons why this argument is incomplete, and point out the inconsistencies in the decoupling procedure. Furthermore, since the results are only as accurate as the consistent averaging approximation, the decoupling approximation is not superior to the consistent averaging method. However, these papers are important since the means by which a reduction in computational intensity may be achieved, without any significant sacrifice in accuracy, was first proposed in them. Further, the persistence of the minimum in the viscosity and first normal stress curves even for very long chains, and the necessity of including FENE springs in order to generate predictions in qualitative agreement with experimental observations in high molecular weight systems, is clearly elucidated in these papers.

4.4. The Gaussian approximation

The closure problem for the second moment equation is solved in the preaveraging assumption of Zimm, and in the self consistent averaging method of Öttinger, by replacing the tensor $\tilde{\mathbf{A}}_{jk}$ with an average. As a result, fluctuations in the hydrodynamic interaction are neglected. The Gaussian approximation [24, 46, 42, 48] makes no assumption with regard to the hydrodynamic interaction, but assumes that the solution of the diffusion equation (81) may be approximated by a Gaussian distribution (67). Since all the complicated averages on the right hand side of the second moment equation (82) can be reduced to functions of the second moment with the help of the Gaussian distribution, this approximation makes it a closed equation for the second moments.

The evolution equation for the covariances σ_{jk} is given by,

$$\begin{aligned} \frac{d}{dt}\sigma_{jk} &= \boldsymbol{\kappa} \cdot \sigma_{jk} + \sigma_{jk} \cdot \boldsymbol{\kappa}^T + \frac{2k_B T}{\zeta} \bar{\mathbf{A}}_{jk} - \frac{H}{\zeta} \sum_m [\sigma_{jm} \cdot \bar{\mathbf{A}}_{mk} + \bar{\mathbf{A}}_{jm} \cdot \sigma_{mk}] \\ &- \frac{H}{\zeta} \frac{H}{k_B T} \sum_{m,l,p} [\sigma_{jl} \cdot \boldsymbol{\Gamma}_{lp,mk} : \sigma_{pm} + \sigma_{mp} : \boldsymbol{\Gamma}_{lp,jm} \cdot \sigma_{lk}] \end{aligned} \quad (88)$$

where, the $(N-1)^2 \times (N-1)^2$ matrix with fourth rank tensor components, $\boldsymbol{\Gamma}_{lp,jk}$, is defined by,

$$\begin{aligned} \boldsymbol{\Gamma}_{lp,jk} &= \frac{3\sqrt{2}h^*}{4} \left[\frac{\theta(j,l,p,k) \mathbf{K}(\hat{\sigma}_{j,k}) + \theta(j+1,l,p,k+1) \mathbf{K}(\hat{\sigma}_{j+1,k+1})}{\sqrt{|j-k|^3}} \right. \\ &- \left. \frac{\theta(j,l,p,k+1) \mathbf{K}(\hat{\sigma}_{j,k+1})}{\sqrt{|j-k-1|^3}} - \frac{\theta(j+1,l,p,k) \mathbf{K}(\hat{\sigma}_{j+1,k})}{\sqrt{|j-k+1|^3}} \right] \end{aligned} \quad (89)$$

while the function $\mathbf{K}(\boldsymbol{\sigma})$ is defined by the equation,

$$\mathbf{K}(\boldsymbol{\sigma}) = \frac{-2}{(2\pi)^{3/2}} \int d\mathbf{k} \frac{1}{k^2} \mathbf{k} \left(\mathbf{1} - \frac{\mathbf{k}\mathbf{k}}{k^2} \right) \mathbf{k} \exp\left(-\frac{1}{2} \mathbf{k} \cdot \boldsymbol{\sigma} \cdot \mathbf{k}\right) \quad (90)$$

The function $\theta(j,l,p,k)$ is unity if l and p lie between j and k , and zero otherwise,

$$\theta(j,l,p,k) = \begin{cases} 1 & \text{if } j \leq l, p < k \quad \text{or} \quad k \leq l, p < j \\ 0 & \text{otherwise} \end{cases} \quad (91)$$

The convention $\mathbf{K}(\hat{\sigma}_{jj})/0 = 0$, has been adopted in equation (89). Both the hydrodynamic interaction functions $\mathbf{H}(\boldsymbol{\sigma})$ and $\mathbf{K}(\boldsymbol{\sigma})$ can be evaluated analytically in terms of elliptic integrals. The properties of these functions are discussed in great detail in the papers by Öttinger and coworkers [22, 24, 25, 48, 47].

All the approximations discussed earlier (with the exception of the decoupling approximation) can be derived by a process of successive simplification of the explicit results for the Gaussian approximation given above. The equations that govern the self consistently averaged theory can be obtained by dropping the last term in equation (88), which accounts for the presence of fluctuations. Replacing $\mathbf{H}(\boldsymbol{\sigma})$ by $\mathbf{1}$ in these truncated equations leads to the governing equations of the Zimm model, while setting $h^* = 0$ leads to the Rouse model.

Material functions predicted by the Gaussian approximation in any arbitrary homogeneous flow may be obtained by solving the system of $(N - 1)^2$ coupled ordinary differential equations for the components of the covariance matrix σ_{jk} (88). Small amplitude oscillatory shear flows and steady shear flow in the limit of zero shear rate have been examined by Öttinger [24] for chains with $N \leq 30$ beads, while Zylka [48] has obtained the material functions in steady shear flow for chains with $N \leq 15$ beads and compared his results with those of Brownian dynamics simulations (the comparison was made for chains with $N = 12$ beads).

The curves predicted by the Gaussian approximation for the storage and loss modulus, G' and G'' , as a function of the frequency ω , are nearly indistinguishable from the predictions of the Zimm theory, suggesting that the Zimm approximation is quite adequate for the prediction of linear visco-elastic properties. There is, however, a significant difference in the prediction of the relaxation spectrum. While the Zimm model predicts a set of $(N - 1)$ relaxation times with equal relaxation weights, the Gaussian approximation predicts a much larger set of relaxation times than the number of springs in the chain, with relaxation weights that are different and dependent on the strength of the hydrodynamic interaction [28]. These results indicate that entirely different relaxation spectrum lead to similar curves for G' and G'' , and calls into question the common practice of obtaining the relaxation spectrum from experimentally measured curves for G' and G'' (see also the discussion in [34]).

The zero shear rate viscosity and first normal stress difference predicted by the Gaussian approximation are found to be smaller than the Zimm predictions for all chain lengths. By extrapolating finite chain length results to the infinite chain limit, Öttinger has shown that this reduction is by a factor of 72% – 73%, independent of the strength of the hydrodynamic interaction parameter. Other universal ratios predicted by the Gaussian approximation in the limit of zero shear rate are discussed later in the chapter.

A comparison of the predicted shear rate dependence of material functions in simple shear flow with the results of Brownian dynamics simulations reveals that of all the approximate treatments of hydrodynamic interaction introduced so far, the Gaussian approximation is the most accurate [48]. Indeed, at low shear rates, the *negative* second normal stress difference predicted by the Gaussian approximation is in accordance with the simulations results.

In spite of the accuracy of the Gaussian approximation, its main drawback is its computational intensity, which renders it difficult to examine chains with large values of N . Apart from the need to examine long chains for the reason cited earlier, it is also necessary to do so in order to obtain the universal predictions of the model. A recently introduced approximation which enables the evaluation of universal viscometric functions in shear flow is discussed in the section below. Before doing so, however, we first discuss the significant difference that a refined treatment of hydrodynamic interaction makes to the prediction of translational diffusivity in dilute polymer solutions.

The correct prediction of the scaling of the diffusion coefficient with molecular weight upon introduction of pre-averaged hydrodynamic interaction in the Zimm model demonstrates the significant influence that hydrodynamic interaction has on the translational diffusivity of the macromolecule. While the pre-averaging assumption appears adequate at equilibrium, it predicts a shear rate independent *scalar* diffusivity even in the presence of a flow field. On the other hand, both the improved treatments of hydrodynamic interaction, namely, consistent averaging and the Gaussian approximation, reveal that the translational diffusivity of a Hookean dumbbell in a flowing homogeneous solution is described by an anisotropic diffusion tensor which is flow rate dependent [23, 26, 27]. Indeed, unlike in the Zimm case, the three different approaches mentioned earlier for calculating the translational diffusivity do not lead to identical expressions for the diffusion tensor [23, 26]. Insight into the origin of the anisotropic and flow rate dependent behavior of the translational diffusivity is obtained when the link between the polymer diffusivity and the shape of the polymer molecule in flow [12] is explored [31, 32]. It is found that the solvent flow field alters the distribution of mass about the centre of the dumbbell. As a consequence, the dumbbell experiences an average friction that is anisotropic and flow rate dependent. The discussion of the influence of improved treatments of hydrodynamic interaction on the translational diffusivity has so far been confined to the Hookean dumbbell model. This is because the concept of the center of resistance, which is very useful for simplifying calculations for bead-spring chains in the Zimm

case, cannot be employed in these improved treatments [23].

4.5. The twofold normal approximation

The twofold normal approximation borrows ideas from the decoupling approximation of Magda *et al.* [18] and Kishbaugh and McHugh [15] in order to reduce the computational intensity of the Gaussian approximation. As in the case of the Gaussian approximation, and unlike in the case of the consistent-averaging and decoupling approximations where it is neglected, fluctuations in the hydrodynamic interaction are included. In a sense, the twofold normal approximation is to the Gaussian approximation, what the decoupling approximation is to the consistent-averaging approximation. The computational efficiency of the decoupling approximation is due both to the reduction in the set of differential equations that must be solved in order to obtain the stress tensor, and to the procedure that is adopted to solve them [33]. These aspects are also responsible for the computational efficiency of the twofold normal approximation. However, the derivation of the reduced set of equations in the twofold normal approximation is significantly different from the scheme adopted in the decoupling approximation; it is more straight forward, and avoids the inconsistencies that are present in the decoupling approximation.

Essentially the twofold normal approximation, (a) assumes that the configurational distribution function ψ is Gaussian, (b) uses the Rouse or the Zimm orthogonal matrix Π_{jk} to map \mathbf{Q}_j to ‘normal’ coordinates \mathbf{Q}'_j , and (c) assumes that the covariance matrix σ_{jk} is diagonalised by the same orthogonal matrix, *ie.* $\sum_{j,k} \Pi_{jp} \sigma_{jk} \Pi_{kq} = \langle \mathbf{Q}'_p \mathbf{Q}'_q \rangle = \sigma'_p \delta_{pq}$. This leads to the following equations for the $(N - 1)$ variances σ'_j ,

$$\frac{d}{dt} \sigma'_j = \boldsymbol{\kappa} \cdot \sigma'_j + \sigma'_j \cdot \boldsymbol{\kappa}^T + \frac{2k_B T}{\zeta} \boldsymbol{\Lambda}_j - \frac{H}{\zeta} \left[\sigma'_j \cdot \boldsymbol{\Lambda}_j + \boldsymbol{\Lambda}_j \cdot \sigma'_j \right] - \frac{H}{\zeta} \frac{H}{k_B T} \sum_k \left[\sigma'_j \cdot \boldsymbol{\Delta}_{jk} : \sigma'_k + \sigma'_k : \boldsymbol{\Delta}_{jk} \cdot \sigma'_j \right] \quad (92)$$

where, $\boldsymbol{\Lambda}_j \equiv \tilde{\boldsymbol{\Lambda}}_{jj}$ are the diagonal tensor components of the matrix $\tilde{\boldsymbol{\Lambda}}_{jk}$,

$$\tilde{\boldsymbol{\Lambda}}_{jk} = \sum_{l,p} \Pi_{lj} \bar{\mathbf{A}}_{lp} \Pi_{pk} \quad (93)$$

and the matrix $\boldsymbol{\Delta}_{jk}$ is given by,

$$\boldsymbol{\Delta}_{jk} = \sum_{l,m,n,p} \Pi_{lj} \Pi_{pk} \boldsymbol{\Gamma}_{lp,mn} \Pi_{mj} \Pi_{nk} \quad (94)$$

In equations (93) and (94), the tensors $\bar{\mathbf{A}}_{jk}$ and $\boldsymbol{\Gamma}_{lp,mn}$ are given by equations (85) and (89), respectively. However, the argument of the hydrodynamic interaction functions is now given by,

$$\hat{\sigma}_{\mu\nu} = \frac{1}{|\mu - \nu|} \frac{H}{k_B T} \sum_{j,k=\min(\mu,\nu)}^{\max(\mu,\nu)-1} \sum_m \Pi_{jm} \Pi_{km} \sigma'_m \quad (95)$$

The decoupling approximation is recovered from the twofold normal approximation when the last term in equation (92), which accounts for fluctuations in hydrodynamic interaction, is dropped. Thus the two different routes for finding governing equations for the quantities σ'_j lead to the same result. However, Prakash and Öttinger [33] have shown that this is in some sense a fortuitous result, and indeed the key assumption made in the decoupling approximation regarding the diagonalisation of $\bar{\mathbf{A}}_{jk}$ is not tenable. The Zimm model in terms of normal modes may be obtained from equation (92) by dropping the last term, and substituting $\tilde{\mathbf{A}}_{jk}$ in place of $\bar{\mathbf{A}}_{jk}$. Of course the Zimm orthogonal matrix must be used to carry out the diagonalisation in equation (93). The diagonalised Zimm model reduces to the diagonalised Rouse model upon using the Rouse orthogonal matrix and on setting $h^* = 0$.

The evolution equations (92) have been solved to obtain the zero shear rate properties for chains with $N \leq 150$, when the Zimm orthogonal matrix is used for the purpose of diagonalisation, and for chains

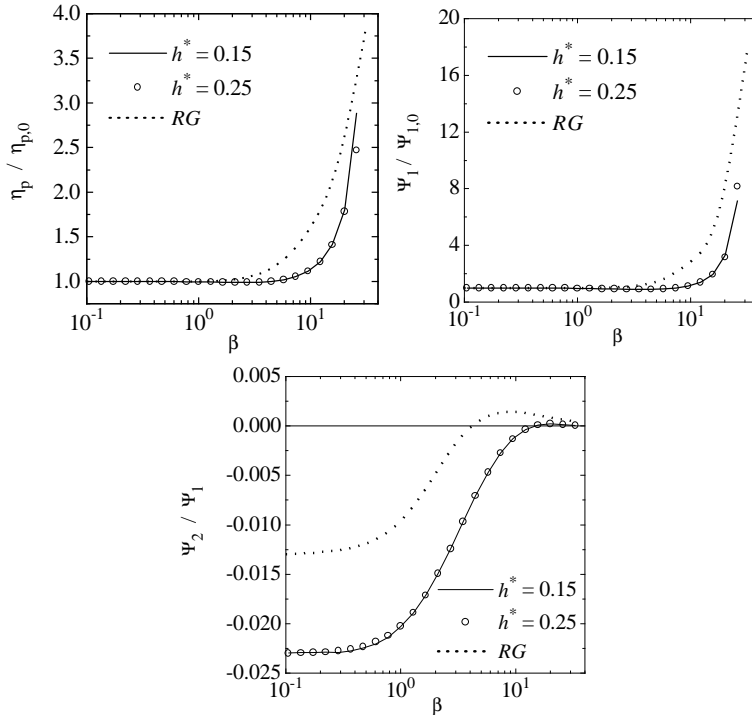


Figure 1. Universal viscometric functions in theta solvents. Reproduced from [33].

with $N \leq 400$, when the Rouse orthogonal matrix is used. Viscometric functions at finite shear rates in simple shear flows have been obtained for chains with $N \leq 100$ [33]. The results are very close to those of the Gaussian approximation; this implies that they must also lie close to the results of exact Brownian dynamics simulations. The reasons for the reduction in computational intensity of the twofold normal approximation are discussed in some detail in [33]. The most important consequence of introducing the twofold normal approximation is that rheological data accumulated for chains with as many as 100 beads can be extrapolated to the limit $N \rightarrow \infty$, and as a result, universal predictions may be obtained.

4.6. Universal properties in theta solvents

One of the most important goals of examining the influence of hydrodynamic interactions on polymer dynamics in dilute solutions is the calculation of universal ratios and master curves. These properties do not depend on the mechanical model used to represent the polymer molecule. Consequently, they reflect the most general consequence of the way in which hydrodynamic interaction has been treated in the theory. They are also the best means to compare theoretical predictions with experimental observations since they are parameter free.

There appear to be two routes by which the universal predictions of models with hydrodynamic interaction have been obtained so far, namely, by extrapolating finite chain length results to the limit of infinite chain length where the model predictions become parameter free, and by using renormalisation group theory methods.

In the former method, there are two essential requirements. The first is that rheological data for finite chains must be generated for large enough values of N so as to be able to extrapolate reliably, *ie.*

Table 1

Universal ratios in the limit of zero shear rate. The exact Zimm values and the Gaussian approximation (GA) values for $U_{\eta R}$ and $U_{\Psi\eta}$ are reproduced from [29], the exact consistent-averaging values from [20], and the renormalisation group (RG) results from [25]. The twofold normal approximation values with the Zimm orthogonal matrix (TNZ) and the remaining GA values are reproduced from [33]. Numbers in parentheses indicate the uncertainty in the last figure.

	$U_{\eta\lambda}$	$U_{\eta R}$	$U_{\Psi\eta}$	$U_{\Psi\Psi}$
Zimm	2.39	1.66425	0.413865	0.0
CA	2.39	1.66425	0.413865	0.010628
GA	1.835 (1)	1.213 (3)	0.560 (3)	-0.0226 (5)
RG	-	1.377	0.6096	-0.0130
TNZ	1.835 (1)	1.210 (2)	0.5615 (3)	-0.0232 (1)

with small enough error, to the limit $N \rightarrow \infty$. The second is that some knowledge of the leading order corrections to the infinite chain length limit must be obtained in order to carry out the extrapolation in an efficient manner. It is clear from the discussion of the various approximate treatments of hydrodynamic interaction above that it is possible to obtain universal ratios in the zero shear rate limit in all the cases. Four universal ratios that are frequently used to represent the rheological behavior of dilute polymer solutions in the limit of zero shear rate are [29],

$$\begin{aligned}
 U_{\eta\lambda} &= \frac{\eta_{p,0}}{nk_B T \lambda_1} & U_{\eta R} &= \lim_{n \rightarrow 0} \frac{\eta_{p,0}}{n\eta_s (4\pi R_g^3/3)} \\
 U_{\Psi\eta} &= \frac{nk_B T \Psi_{1,0}}{\eta_{p,0}^2} & U_{\Psi\Psi} &= \frac{\Psi_{2,0}}{\Psi_{1,0}}
 \end{aligned} \tag{96}$$

where, λ_1 is the longest relaxation time, and R_g is the root-mean-square radius of gyration at equilibrium. With regard to the leading order corrections to these ratios, it has been possible to obtain them explicitly only in the consistently-averaged case [20]. In both the Gaussian approximation and the twofold normal approximation it is assumed that the leading order corrections are of the same order, and extrapolation is carried out numerically by plotting the data as a function of $(1/\sqrt{N})$. Because of their computational intensity, it is not possible to obtain the universal shear rate dependence of the viscometric functions predicted by the consistent-averaging and Gaussian approximations. However, it is possible to obtain these master curves with the twofold normal approximation.

Table 1 presents the prediction of the universal ratios (96) by the various approximate treatments. Miyaki *et al.* [19] have experimentally obtained a value of $U_{\eta R} = 1.49$ (6) for polystyrene in cyclohexane at the theta temperature. Figure 1 displays the viscometric functions predicted by the two fold normal approximation. The coincidence of the curves for the different values of h^* indicate the parameter free nature of these results. Divergence of the curves at high shear rates implies that the data accumulated for chains with $N \leq 100$ is insufficient to carry out an accurate extrapolation at these shear rates. The incorporation of the effect of hydrodynamic interaction into kinetic theory clearly leads to the prediction of shear thickening at high shear rates even in the long chain limit.

In both table 1 and figure 1, the results of renormalisation group calculations (RG) are also presented [25, 47]. As mentioned earlier, the renormalisation group theory approach is an alternative procedure for obtaining universal results. It is essentially a method for refining the results of a low-order perturbative treatment of hydrodynamic interaction by introducing higher order effects so as to remove the ambiguous definition of the bead size. All the infinitely many interactions for long chains are brought in through the idea of self-similarity. It is a very useful procedure by which a low-order perturbation result, which can account for only a few interactions, is turned into something meaningful. However, systematic results can only be obtained near four dimensions, and one cannot estimate the errors in three dimensions reliably.

The Gaussian and twofold normal approximations on the other hand are non-perturbative in nature, and are essentially ‘uncontrolled’ approximations with an infinite number of higher order terms.

It is clear from the figures that the two methods lead to significantly different results at moderate to high shear rates. A minimum in the viscosity and first normal stress difference curves is not predicted by the renormalisation group calculation, while the twofold normal approximation predicts a small decrease from the zero shear rate value before the monotonic increase at higher shear rates. The good comparison with the results of Brownian dynamics simulations for short chains indicates that the twofold normal approximation is likely to be more accurate than the renormalisation group calculations.

5. CONCLUSIONS

This chapter discusses the development of a unified basis for the treatment of non-linear microscopic phenomena in molecular theories of dilute polymer solutions and reviews the recent advances in the treatment of hydrodynamic interaction. In particular, the successive refinements which ultimately lead to the prediction of universal viscometric functions in theta solvents have been highlighted.

REFERENCES

- [1] R. B. Bird, R. C. Armstrong and O. Hassager, Dynamics of Polymeric Liquids, Vol. 1, Fluid Mechanics, 2nd edn., John Wiley, 1987.
- [2] R. B. Bird, C. F. Curtiss, R. C. Armstrong and O. Hassager, Dynamics of Polymeric Liquids, Vol. 2, Kinetic Theory, 2nd edn., John Wiley, 1987.
- [3] R. B. Bird and H. C. Öttinger, Annu. Rev. Phys. Chem., 43, (1992) 371-406.
- [4] C. F. Curtiss and R. B. Bird, Adv. Polymer Sci., 125, (1996), 1-101.
- [5] C. F. Curtiss, R. B. Bird and O. Hassager, Adv. Chem. Phys., 35 (1976) 31-117.
- [6] J. des Cloizeaux and G. Jannink, Polymers in Solution, Their Modelling and Structure, Oxford Science Publishers, 1990.
- [7] P-G. de Gennes, Scaling Concepts in Polymer Physics, Cornell University Press, 1979.
- [8] M. Doi and S. F. Edwards, The Theory of Polymer Dynamics, Clarendon Press, Oxford, 1986
- [9] X. J. Fan, J. Non-Newtonian Fluid Mech., 17 (1985) 125-144.
- [10] X. J. Fan, J. Chem. Phys., 85 (1986) 6237-6238.
- [11] M. Fixman, J. Chem. Phys., 45 (1966) 785-792, 793-803.
- [12] D. A. Hoagland and R. K. Prud'homme, J. Non-Newtonian Fluid Mech., 27 (1988) 223-243.
- [13] J. G. Kirkwood, Macromolecules, Gordon and Breach, New York, 1967
- [14] J. G. Kirkwood and J. Riseman, J. Chem. Phys., 16 (1948) 565-573.
- [15] A. J. Kishbaugh and A. J. McHugh, J. Non-Newtonian Fluid Mech., 34 (1990) 181-206.
- [16] H. A. Kramers, Physica, 11 (1944) 1-19.
- [17] R. G. Larson, Constitutive Equations for Polymer Melts and Solutions, Butterworths, Boston, 1988.
- [18] J. J. Magda, R. G. Larson and M. E. Mackay, J. Chem. Phys., 89 (1988) 2504-2513.
- [19] Y. Miyaki, Y. Einaga, H. Fujita and M. Fukuda, Macromolecules, 13 (1980) 588.
- [20] H. C. Öttinger, J. Chem. Phys., 86 (1987) 3731-3749.
- [21] H. C. Öttinger, J. Chem. Phys., 87 (1987) 3156-3165.
- [22] H. C. Öttinger, J. Non-Newtonian Fluid Mech., 26 (1987) 207-246.
- [23] H. C. Öttinger, J. Chem. Phys., 87 (1987) 6185-6190.
- [24] H. C. Öttinger, J. Chem. Phys., 90 (1989) 463-473.
- [25] H. C. Öttinger and Y. Rabin, J. Non-Newtonian Fluid Mech., 33 (1989) 53-93.
- [26] H. C. Öttinger, AIChE J., 35 (1989) 279-285.
- [27] H. C. Öttinger, Coll. Polym. Sci., 267 (1989) 1-8.
- [28] H. C. Öttinger and W. Zylka, J. Rheol., 36 (1992) 885-910.
- [29] H. C. Öttinger, Stochastic Processes in Polymeric Fluids, Springer-Verlag, 1996.
- [30] H. C. Öttinger, Rheologica Acta, 35 (1996) 134-138.
- [31] J. R. Prakash and R. A. Mashelkar, J. Chem. Phys., 95 (1991) 3743-3748.

- [32] J. R. Prakash and R. A. Mashelkar, *J. Rheol.*, 36 (1992) 789-805.
- [33] J. R. Prakash and H. C. Öttinger, *J. Non-Newtonian Fluid Mech.*, 71 (1997) 245-272.
- [34] J. R. Prakash, in: M. J. Adams, R. A. Mashelkar, J. R. A. Pearson and A. R. Rennie (Eds.), *Dynamics of Complex Fluids*, Imperial College Press–The Royal Society, 1998.
- [35] Y. Rabin and H. C. Öttinger, *Euro-Phys. Lett.*, 13 (1990) 423-428.
- [36] P. E. Rouse, *J. Chem. Phys.*, 21 (1953) 1272-1280.
- [37] J. D. Schieber and H. C. Öttinger, *J. Chem. Phys.*, 89 (1988) 6972-6981.
- [38] J. D. Schieber, *J. Rheol.*, 37 (1993) 1003-1027.
- [39] J. D. Schieber and H. C. Öttinger, *J. Rheol.*, 38 (1994) 1909-1924.
- [40] G. Strobl, *The Physics of Polymers*, Springer-Verlag, 1996.
- [41] L. E. Wedgewood and H. C. Öttinger, *J. Non-Newtonian Fluid Mech.*, 27 (1988) 245-264.
- [42] L. E. Wedgewood, *J. Non-Newtonian Fluid Mech.*, 31 (1989) 127-142.
- [43] L. E. Wedgewood, *Rheol. Acta*, 32 (1993) 405-417.
- [44] H. Yamakawa, *Modern Theory of Polymer Solutions*, Harper & Row, New York, 1971.
- [45] B. H. Zimm, *J. Chem. Phys.*, 24 (1956) 269-281.
- [46] W. Zylka and H. C. Öttinger, *J. Chem. Phys.*, 90 (1989) 474-480.
- [47] W. Zylka and H. C. Öttinger, *Macromolecules*, 24 (1991) 484-494.
- [48] W. Zylka, *J. Chem. Phys.*, 94 (1991) 4628-4636.